Osteoblast Response to Zirconia-Hybridized Pyrophosphate Stabilized Amorphous Calcium Phosphate

Bryce Matthew Whited

Thesis submitted to the faculty of the Virginia Polytechnic Institute and State University
in partial fulfillment of the requirements for the degree of

Master of Science
in
Biomedical Engineering

Brian J. Love, Co-Chair
Aaron S. Goldstein, Co-Chair
John R. Cotton

May 4th, 2005
Blacksburg, VA

Keywords: Bone tissue engineering, osteoblast, differentiation, osteogenesis, polylactic acid, calcium phosphate

Osteoblast Response to Zirconia-Hybridized Pyrophosphate Stabilized Amorphous Calcium Phospate

Bryce M. Whited

(Abstract)

Biodegradable polyesters, such as poly(DL-lactic-co-glycolic acid) (PLGA), have been used to fabricate porous bone scaffolds to support bone tissue development. These scaffolds allow for cell seeding, attachment, growth and extracellular matrix production in vitro and are replaced by new bone tissue when implanted into bone sites in vivo. Hydroxyapatite (HAP) and β-tricalcium phosphate (β-TCP) ceramics have been incorporated into PLGA bone scaffolds and have been shown to increase their osteoconductivity (support cell attachment). Although HAP, β-TCP, and biodegradable polyesters are osteoconductive, there is no evidence that these scaffold materials are osteoinductive (support cell differentiation). Calcium and phosphate ions, in contrast, have been postulated to be osteogenic factors that enhance osteoblast differentiation and mineralization. Recently, a zirconia-hybridized pyrophosphate stabilized amorphous calcium phosphate (Zr-ACP) has been synthesized which permits controlled release of calcium and phosphate ions and thus is hypothesized to be osteoinductive. Incorporation of Zr-ACP into a highly porous poly(DL lactic-co-glycolic acid) (PLGA) scaffold could potentially increase the osteoinductivity of the scaffold and therefore promote osteogenesis when implanted in vivo.

To determine the osteoinductivity of Zr-ACP, a MC3T3-E1 mouse calvarial-derived osteoprogenitor cell line was used to measure cell response to Zr-ACP. To accomplish this objective, Zr-ACP was added to cell culture at different stages in cell maturation (days 0, 4 and 11). DNA synthesis, alkaline phosphatase (ALP) activity,

osteopontin synthesis and collagen synthesis were determined. Results indicate that culture in the presence of Zr-ACP significantly increased cell proliferation, ALP activity and osteopontin synthesis but not collagen synthesis. To determine the feasibility of incorporating Zr-ACP into a PLGA scaffold, PLGA/Zr-ACP composite foams (5% or 10% (w/v) polymer:solvent with 25 wt% or 50 wt% Zr-ACP) were fabricated using a thermal phase inversion technique. Scanning electron microscopy revealed a highly porous structure with pores ranging in size from a few microns to about 100 μm. The amorphous structure of the Zr-ACP was maintained during composite fabrication as confirmed by X-ray diffraction measurements. Composite scaffolds also showed significantly greater compressive yield strengths and moduli as compared to pure polymer scaffolds.

The results of this study indicate that Zr-ACP enhances the osteoblastic phenotype of MC3T3-E1 cells in vitro and can be incorporated into a porous PLGA scaffold. Porous PLGA/Zr-ACP composites are promising for use as bone scaffolds to heal bone defects.

Acknowledgements

I would first like to thank my advisors and other professors at Virginia Tech who have assisted me with my thesis research. I would like to thank my advisor, Dr. Brian Love, for his countless hours of guidance and patience throughout my graduate career. My thanks go to Dr. Aaron Goldstein for his instruction on experimental setup and technical writing. I am also grateful to Dr. John Cotton for serving on my graduate committee. Their insight and guidance has been invaluable in my development as a researcher.

I would also like to thank my fellow graduate student, Michelle Kreke, for assistance with cell culture work and protein analysis. Without her help, I would not have been able to complete the majority of laboratory work for my graduate research. I am greatly indebted to her.

Finally, I would like to thank my family and friends for their love and support. I am grateful to my friends for helping me to keep my sanity during my graduate career. I would like to thank my brothers, Brad, Brett and Brant Whited, for their loyalty and for being the best friends I could ever have. To my parents, Roger and Connie Whited, I am grateful for their never-ending love, support and encouragement. Above all, I would like to thank God for faithfully loving, directing and guiding me on this journey of life.

Table of Contents

List of Figures

Chapter 1

Chapter 2

Chapter 3

List of Tables

Chapter 1

Chapter 3

Chapter 1: Introduction

1.1 Conventional bone replacement and regeneration techniques

There are nearly 1 million cases of skeletal defects a year that require bone graft procedures to achieve union or to fill bone voids [1]. These numbers are expected to increase substantially within the next few years due to an aging population [1]. Current treatments for bone replacement and regeneration are based on autologous bone grafts (autografts) [2], allogenic bone grafts (allografts) [3] or, as an alternative to these, metals and ceramics [2].

Autografts, taken from another part of the patient's own body, have been the gold standard for years because they provide osteogenic cells as well as essential osteoinductive factors needed for bone healing and regeneration [2]. They are commonly trabecular bone from the patients own iliac crest, but cortical bone can be used as well depending on defect size, shape and application [4]. Although autografts are successful their use is limited, mainly due to the volume of bone available and concerns of donor site morbidity [5].

Allografts, taken from a donor's body (usually cadavers), are an alternative. However, graft incorporation is substantially lower than with the autograft [3]. Furthermore, allografts introduce the possibility of immune rejection and pathogen transmission from donor to host, and subsequently infections could occur in the recipient's body after transplantation [3].

In addition to these two bone grafts, metals and ceramics are an alternative, although both materials present several disadvantages [2]. Metals provide immediate

mechanical stability at the site of the defect, although, they exhibit very poor integration with the tissue and can fail because of infection, fatigue loading and bone resorption [1]. Ceramics have a low tensile strength are usually very brittle thus they cannot be used in locations of significant bending, torsion or shear stress [2]. A limited number of ceramics, alternatively, are very well suited for bone grafts and will be discussed later in this chapter.

Hence adequate bone replacements are still being sought and are urgently needed for patient recovery from bone defects or injury. A possible solution for these problems may be found with bone tissue engineering. Bone tissue engineering can be defined as the application of biological, chemical and engineering principles toward the repair, restoration or regeneration of living bone tissue [6]. The approaches for bone tissue engineering involve using one or more of the following key ingredients: three dimensional matricies (scaffolds), harvested cells and recombinant signaling molecules [6]. Ideally, seeded cells would attach to the scaffold and proliferate and differentiate under the control of endogenous and exogenous growth factors in vitro. This scaffold, when implanted into the patient, would degrade and eventually be replaced by natural bone tissue [6].

1.2 Bone scaffolds – temporary matrices for bone growth

To restore bone function or regenerate bone tissue, a scaffold is needed that will act as a temporary matrix for cell proliferation and extracellular matrix (ECM) deposition, with subsequent bone in-growth until the new bony tissue is totally restored/regenerated (Figure 1) [7]. In addition, bone scaffolds provide cells with a tissue

specific environment and architecture and serve as a reservoir for water, nutrients, cytokines and growth factors [6].

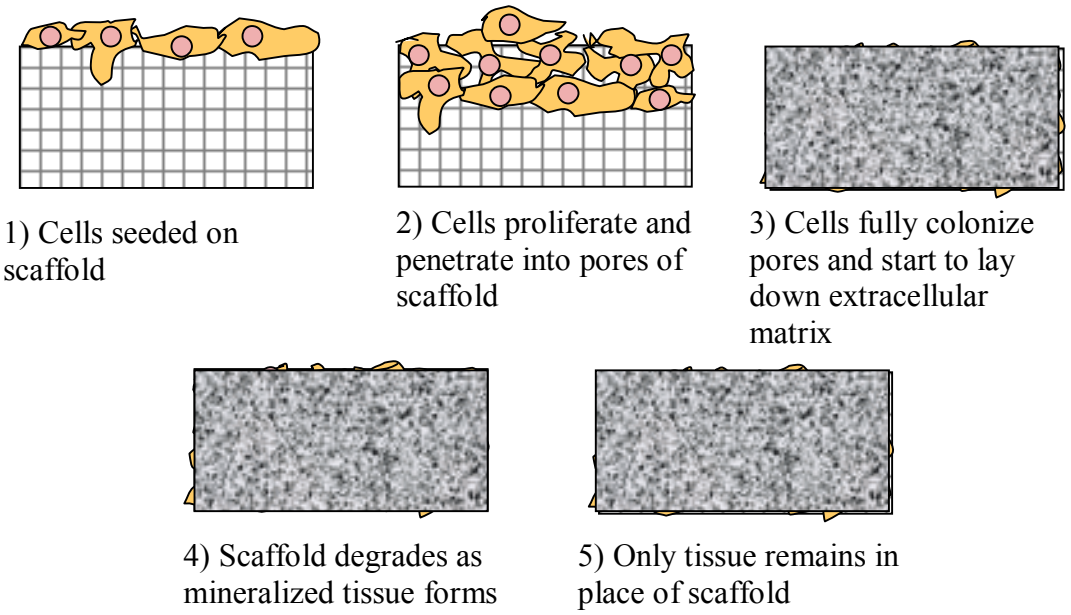

Figure 1: Diagram of bone scaffold seeding, tissue ingrowth and resorption.

Bone scaffolds must have an array of biological specific and morphological properties that make them suitable for bone regeneration. Besides the choice of adequate materials (addressed later), attributes such as porosity, pore size, surface texture, mechanical properties , biocompatibility and biodegradability, are of extreme importance (Figure 2) [8]. These properties affect not only cell survival, signaling and growth, but also gene expression and phenotype [8].

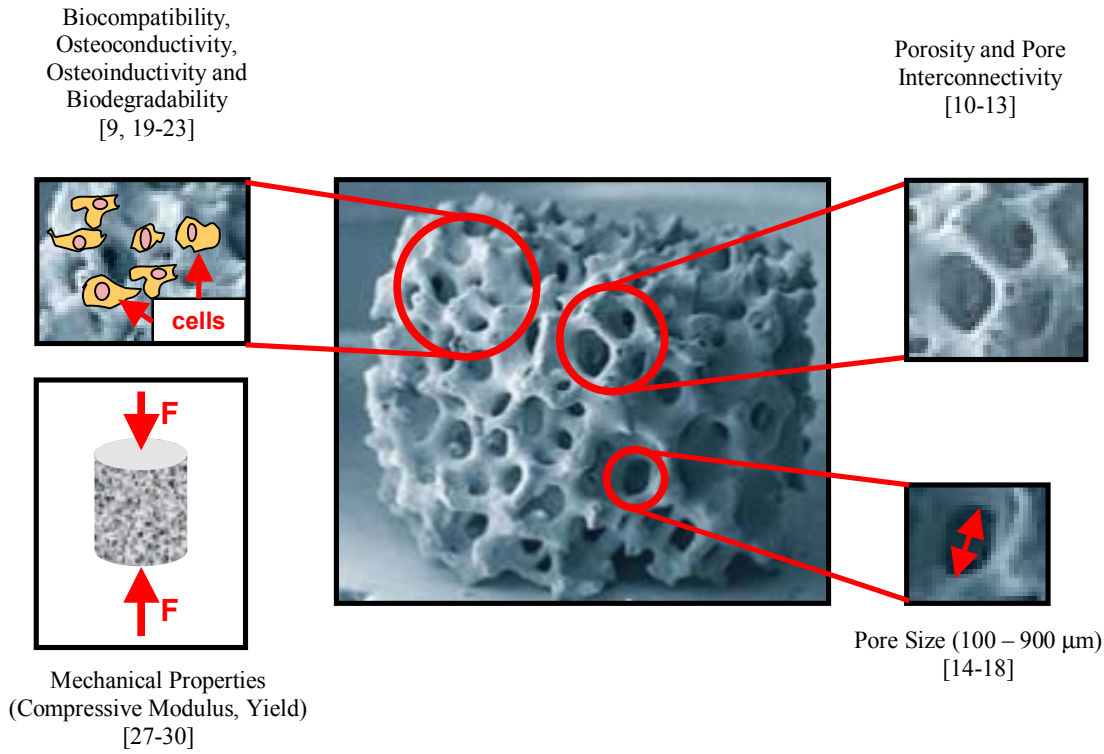

Figure 2: Schematic diagram of bone scaffold and desired properties (Image from Salgado et. al. [111])

1.3 Essential bone scaffold properties

The following properties have been defined as being essential for bone tissue scaffolds [11-25]:

1.3.1 Biocompatibility

Scaffolds should be able to integrate into the host tissue without eliciting an immune response [9]. The degradation byproducts of the scaffold must also be biocompatible.

1.3.2 Porosity

Interconnecting pores are necessary for bone tissue formation because they allow tissue ingrowth as well as vascularization [10]. In addition, a porous surface improves mechanical interlocking between the implant biomaterial and the surrounding natural bone, providing greater mechanical stability at this critical interface [11]. However, the degree of porosity always influences other properties of the scaffolds such as its mechanical stability. In light of this, porosity should always be balanced with the mechanical needs of the particular tissue that is going to be replaced [12]. A target porosity range of 75% to 90% has been suggested for bone scaffolds in vivo, although such highly porous scaffolds limit uses in vivo that require load bearing [13].

1.3.3 Pore size

The minimum useful pore size for a scaffold is 100 μm based on the work of Itala et al. [14]. Subsequent studies have shown better osteogenesis in vitro for implants with pores ranging from 300 μm to 900 μm [15-17]. Larger pore sizes favor direct osteogenesis in vivo, since they allow vascularization and higher oxygenation [18]. Smaller pores result in osteochondral ossification in vivo, although the type of bone ingrowth depends on the biomaterial and pore geometry [18].

1.3.4 Osteoconductivity

The topographical and chemical surface properties of the biomaterial can control and affect osteoconduction [19]. Osteoconduction refers to the ability of a material to serve as a substrate onto which bone cells can attach, migrate, and grow and divide. It

has been previously shown that relatively rougher surfaces facilitate cellular attachment and subsequent osteoblastic migration [20]. Surface chemistry of the scaffold also plays a role in osteoconduction. As an example, surface chemistry of poly(α-hydroxy ester) scaffolds, specifically the addition of hydrophilic poly(ethylene glycol) (PEG), has been demonstrated to decrease attachment but increase differentiation of seeded osteoblasts [21]. Addition of peptides [22] and increase in positive surface charge [23] have also been shown to increase the osteoconductivity of surfaces.

1.3.5 Osteoinductivity

Osteoinduction is the process of osteoprogenitor cell recruitment to a bone healing site and subsequent differentiation to the osteoblastic phenotype [20]. Scaffolds that exhibit only osteoconductivity may be suitable for small defects, but larger defects may benefit from osteoinductive factors evolved directly from the scaffold to aid in bone regeneration [20]. Osteoinductive factors that have been integrated into bone scaffolds include a number of bone-related growth factors, including insulin-like growth factor, fibroblast growth factor, platelet-derived growth factor, and members of the transforming growth factor-β family (specifically bone morphogenic proteins) which regulate osteoblast function [24-26].

1.3.6 Mechanical properties and biodegradability

In vivo, the bone scaffold should have sufficient mechanical strength to withstand hydrostatic pressures and to maintain porosity/pore structure to facilitate cell invasion, extracellular matrix production and bone ingrowth [8]. If the scaffold is load bearing,

then the mechanical properties of the scaffold should match the properties of the bone that it is replacing: elastic moduli of about 20 GPa – 120 GPa for cortical bone [27, 28] and about 50 MPa – 300 MPa for trabecular bone [28, 29]. Furthermore, the degradation rate of the scaffold should be tuned appropriately with the growth rate of new tissue, in such a way that by the time the injury site is remodeled the scaffold is totally degraded to allow neo-tissue ingrowth [30].

1.4 Biomaterials used for bone scaffolds

The material chosen for a bone scaffold is very important because it must possess or be able to be modified to achieve adequate biocompatibility, porosity, pore size, surface texture, mechanical properties and biodegradability. To date, ceramics and polymers from both natural and synthetic origins have been used to construct bone scaffolds for bone defects (Table 1). However, most ceramics are not biodegradable, which presents a problem in bone restoration applications that require the scaffold material to degrade over time. This limits scaffold material choices to a small number of ceramics and biodegradable polymers.

Table 1: Bone scaffold materials and observations in vitro

Materials	Observations	Ref.
Hydroxyapatite (HAP)	• Good cell attachment and ECM production • Not bioresorbable	[31]
Beta-Tricalcium Phosphate (β-TCP)	• Good cell attachment, differentiation and mineralization in vitro • Somewhat bioresorbable relative to HAP	[32]
Poly(DL-lactic-co-glycolic acid) (PLGA)	• Support cell attachment, differentiation, ECM production while scaffold degrades • Scaffold degradation controlled by co-polymer ratio	[15, 33, 34]
PLGA-HAP composite	• Greater cell differentiation and mineralization than PLGA scaffold alone • Semi-bioresorbable	[35]
Alginate	• Cell proliferation with no cytotoxicity • Bioresorbable	[36]
Chitosan	• Good cell attachment and differentiation • Not bioresorbable	[37]
Fibrin	• Support cell attachment and mineralization • Bioresorbable	[38]

1.4.1 Ceramics

Ceramics, such as hydroxyapatite, bioactive glasses and calcium phosphates, have been widely used for bone regeneration and replacement [39]. All three materials exhibit a bioactive and biocompatible behavior and have been traditionally used as coatings on metals for orthopedic/dental implants but more recently have been proposed as filler material for bone defects and as bone scaffolds [39]. These materials are unique in that

they form a calcium-deficient (non-stochiometric) apatite surface layer in the presence of biological fluids [40]. This surface layer is thought to stimulate bioceramic-bone binding and, in some cases, promote new bone formation [41].

Calcium phosphate based materials, in particular, have been widely investigated for use as bone replacement materials due to their biocompatibility and osteoconductivity [32, 35, 42-44]. Synthetic hydroxyapatite (HAP) and β-tricalcium phosphate (β-TCP) are the two most common calcium phosphate materials used as hard-tissue replacements [7]. Several studies have shown that using these two bioceramics as bone scaffolds, both seeded with and seeded without bone marrow cells, have yielded bone regeneration [31, 45-47].

Amorphous calcium phosphates have been used sparingly as bone replacements, mainly because of rapid and uncontrolled dissolution [48, 49]. Recently, amorphous calcium phosphate has been stabilized by pyrophosphate ions ($P_2O_7^{-4}$) and hybridized with zirconium (Zr-ACP) to retard its dissolution and subsequent conversion to HAP in aqueous environments [50, 51]. In addition, Zr-ACP allows for controlled release of calcium and phosphate ions; factors that have been postulated to increase osteoblast differentiation and mineralization in vitro [52-55].

Calcium phosphates are biocompatible and osteoconductive, although they have some drawbacks for use as bone scaffolds. These materials are brittle and have low mechanical stability, which limits their use in large defects that require load bearing [41]. Furthermore, their dissolution and degradation rates are difficult to control in vivo [41]. These factors could present a problem because if the scaffold degrades too fast, the mechanical stability would be compromised and could fail.

1.4.2 Biodegradable polymers

Biodegradable polymers are a promising alternative to ceramics for bone tissue scaffolds. Biodegradable polymers allow cell adhesion, support bone tissue regeneration, degrade slowly into non-toxic byproducts and possess adequate mechanical stability to support and transfer loads known to exist in bone [56, 57]. Biodegradable polymers for tissue engineering are classified into two groups: natural and synthetic. Some commonly used biodegradable polymers and their origin and characteristics are listed in Table 2. Natural biodegradable polymers are those obtained from plant or animal sources. The main advantages of these materials are their good osteoconductivity, low immunogenic response in vivo and high availability.

Table 2: Natural and synthetic biodegradable polymers used for bone tissue engineering

Material	Origin	Characteristics	References
Fibrin	Natural	• Promotes osteoconduction • Promotes cell migration and vascularization	[38]
Chitosan	Natural	• Promotes osteoconduction and wound healing	[58-60]
Collagen	Natural	• Low immune response • Good substrate for cell adhesion • Chemotactic	[61-63]
Starch	Natural	• Thermoplastic behavior • Good substrate for cell adhesion • Non-cytotoxic and biocompatible • Scaffolds including this material have good mechanical properties	[64, 65]
Poly(α-hydroxy acids)	Synthetic	• Degradation by hydrolysis • FDA approved • Byproducts (e.g. lactic acid, glycolic acid) are metabolized or excreted • Can present problems in area of implantation due to decrease in local pH	[15-17, 66, 67]
Poly(propylene fumarates)	Synthetic	• Main degradation products are metabolized and excreted • Good biocompatibility	[68, 69]
Poly(ε-caprolactone)	Synthetic	• Aliphatic polyester • Slow degrading • Degraded by hydrolysis or bulk erosion • Some problems related to sustained mechanical loads (creep)	[70-73]
Poly(anhydrides)	Synthetic	• Developed for drug delivery carriers • Biocompatible	[74]

Synthetic biodegradable polymers, such as poly(L-lactic acid) (PLLA), poly(glycolic acid) (PGA) and poly(DL-lactic-co-glycolic acid) (PLGA) copolymer

(Figure 3) have been used extensively for bone tissue scaffolds because they are osteoconductive and can degrade in vivo to allow new bone tissue ingrowth [15-17].

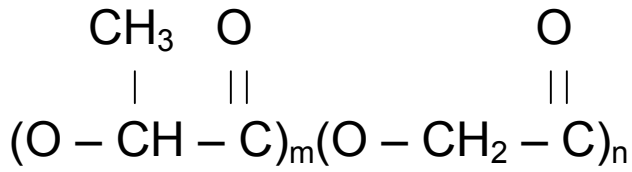

Figure 3: Chemical structure of PLGA copolymer

PLGA copolymer degradation can range from a few weeks to years depending on the copolymer ratio, crystallinity and molecular weight [15]. The degradation byproducts of PLGA can be eliminated from the body through either the citric acid cycle or renal excretion [15]. PLGA can also be processed into three dimensional porous structures suitable for treatment of bone tissue defects. Two drawbacks of these materials are the release of non-degraded PLLA microparticles that cause foreign body inflammatory reactions and acidic degradative byproducts that decrease local pH which stimulates bone resorption [75].

1.4.3 Composites

PLGA and PLLA have been combined with HAP and β-TCP to form biodegradable polymer/ceramic composites with the goal of increasing osteoconductivity, buffering acidic byproducts and increasing the compressive modulus of the pure polymeric materials [76-78]. One such porous scaffold comprised of PLGA and β-TCP, seeded with mesenchymal stem cells, was cultivated in osteogenic medium over a 40 day period resulting in increased collagen type I and osteocalcin in the scaffold as compared

to the PLGA scaffold alone [76]. This study confirmed that cell attachment, proliferation and ECM production was increased with addition of β-TCP to the PLGA scaffold. In a similar study, PLLA was combined with ossein, a biological HAP, seeded with osteoblast precursor cells, and was tested to determine thermal, morphological, mechanical and osteoconductivity properties of the composites [77]. Compressive modulus of the composite scaffold was greater than the PLLA scaffold and a greater osteoblast phenotypic response was seen with the composite as compared to the PLLA scaffold [77].

Because some polymeric scaffolds may not be strong enough to stabilize large bone fractures, absorbable high-strength calcium phosphate glass fibers are being developed for incorporation into biodegradable polymers [78]. Such biodegradable polymer/calcium phosphate composites showed good biocompatibility and no inflammation after 9 weeks of implantation in rabbit tibiae, which shows potential in vivo [78].

1.5 Scaffold fabrication techniques

Several techniques have been developed to process both synthetic and natural polymeric scaffold materials into continuous, interconnected porous structures. These conventional scaffold fabrication techniques include solvent casting-particulate leaching [66, 79], gas foaming [17], fiber meshes/fiber bonding [80, 81], melt molding [82, 83], and thermal phase separation/freeze drying [36, 37, 84-89].

1.5.1 Solvent casting/particulate leaching

Solvent casting/particulate leaching involves using a solution of PLLA in chloroform and adding salt particles of a specific diameter to produce a uniform suspension [66]. The solvent is allowed to evaporate leaving behind a polymer matrix with salt particles embedded throughout. The composite is then immersed in water where the salt leaches out to produce a porous structure. Pore diameters ranging from 100-500 μm and porosities of 87-91% have been obtained using this method [66]. In addition, a lamination technique using chloroform as the binder has been proposed to shape these scaffolds into 3D structures [79].

Scaffolds produced by solvent-casting particulate-leaching cannot guarantee pore interconnectivity because this depends on whether the adjacent salt particles are in contact [90]. Furthermore, skin layers are formed during evaporation and agglomeration of salt particles makes controlling the pore size difficult [90]. Moreover, only thin scaffold cross-sections can be produced due to the difficulty in removing salt particles deep in the matrix [90].

1.5.2 Gas foaming

For gas foaming, a biodegradable polymer, such as PLGA is saturated with carbon dioxide (CO_2) at high pressures where after the pressure is decreased to atmospheric levels [17]. This results in nucleation and growth of gas bubbles with sizes ranging between 100- 500 μm in the polymer. A drawback to this method is that only 10-30% of the pores in the structure are interconnected [17].

1.5.3 Fiber meshes/fiber bonding

Fibers, produced by textile technology, have been used to make non-woven scaffolds from PGA and PLLA [80]. The lack of structural stability of these non-woven scaffolds often results in significant shrinkage due to contractile forces of the cells that have been seeded into the scaffold [80]. This has led to the development of a fiber bonding technique to increase the mechanical properties of the scaffolds [81]. Bonding is achieved by dissolving PLLA in methylene chloride and casting over the PGA mesh. The solvent is allowed to evaporate and the construct is then heated above the melting point of both polymers. Once the PGA-PLLA construct has cooled, the PLLA is removed by dissolving in methylene chloride again. Fiber bonding results in a mesh of PGA fibers joined at the cross-points [81].

1.5.4 Melt molding

Melt molding involves filling a teflon mold with PLGA and porogen (e.g. gelatin microspheres, salt crystals) and then heating the mold above the glass transition temperature of PLGA while applying pressure [82]. This method causes the PLGA particles to bond and then the porogen is leached out with water. This method was modified to incorporate short HAP fibers to increase the structural stability of the scaffold which had 93% porosity with 100 μm interconnected pores [83].

1.5.5 Temperature induced phase separation/freeze drying

Temperature induced phase separation (TIPS)/freeze drying involves dissolving a polymer into a solvent at an elevated temperature and then decreasing the temperature of

the solution to induce a polymer-rich/polymer lean phase separation. Subsequent sublimation of the solvent results in formation of a porous structure (Figure 4) [84].

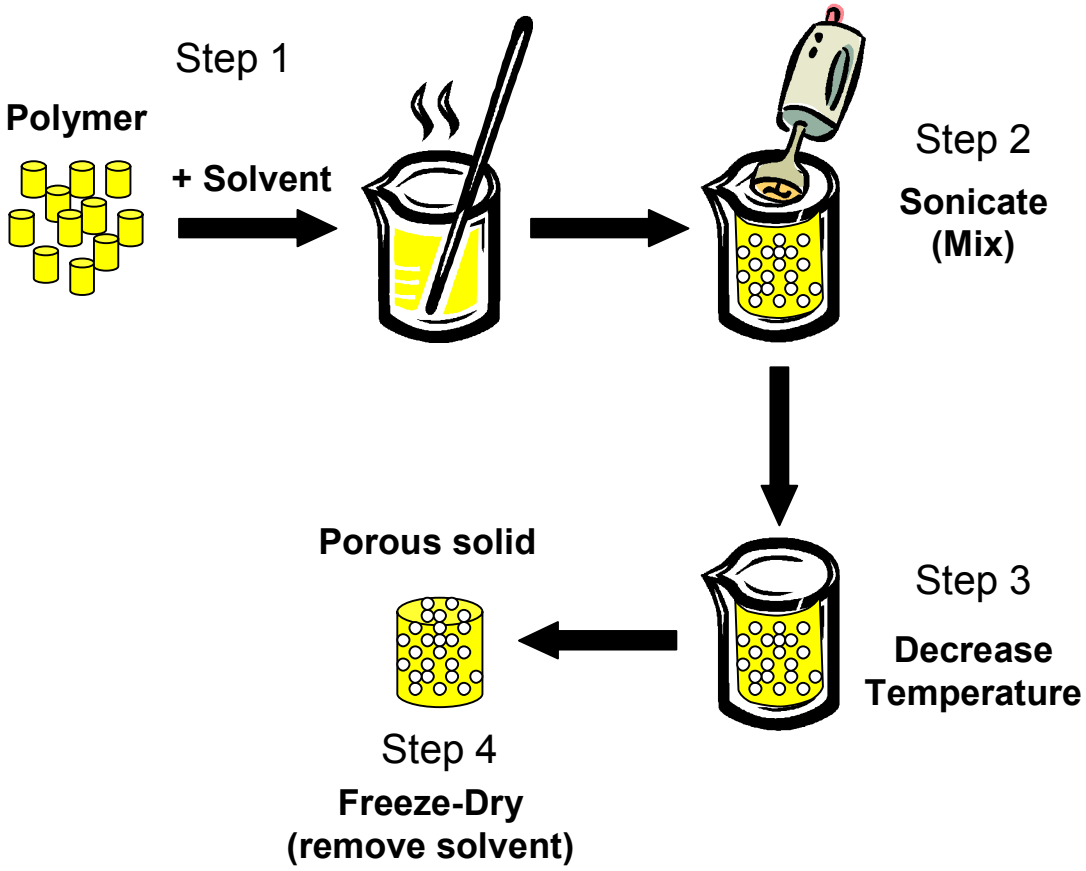

Figure 4: Fabrication of porous polymer scaffold via thermal phase inversion

Synthetic polymers, such as PLGA, can be dissolved in dioxane, benzene or other solvents. The pore size can be controlled by the freezing rate and pH; a fast freezing rate produces smaller pores [85, 86]. TIPS/freeze drying has been used to create a homogenous 3D-pore structure [87, 88]. This method retains water-soluble agents during scaffold fabrication that would otherwise be eliminated during solvent casting/leaching methods [84]. Other natural polymers like collagen [89], chitosan [37] and alginate [36]

have been fabricated into scaffolds using the TIPS/freezing-drying method. Some disadvantages of this method include low compressive modulus, formation of skins and limited interconnectivity of pores [9].

1.6 Cells for bone tissue engineering

Osteoblasts are the skeletal cells responsible for synthesis, deposition, and mineralization of the extracellular matrix of bone [91]. By mechanisms that are only beginning to be understood, osteoprogenitor cells and related mesenchymal precursor cells arise in the embryo and at least some appear to persist in the adult organism, where they contribute to osteoblast replacement in bone remodeling or fracture healing [91]. Since osteoprogenitor cells are naturally found at bone healing sites in vivo, it is logical that they be included (or seeded) into bone tissue scaffolds to increase the healing potential in the defect. Osteoprogenitor cells have been used for bone tissue engineering in two ways. The first method is to seed osteoprogenitor cells into bone scaffolds and then implant them at the defect sites. The second method involves in vitro culture of the osteoprogenitor cells within the scaffold under conditions that induce osteoblastic differentiation and bone-like tissue development followed by implantation of the scaffold at the defect site. Both methods provide the scaffold with osteoinductive factors that allow the structure to increase healing at the defect site.

1.6.1 Mesenchymal stem cells

In the bone tissue engineering field, there has been special interest in adult stem cells known as mesenchymal stem cells (MSC). Although a true mesenchymal stem cell

(MSC) with capacity for indefinite self-renewal and potential to form into all tissue types has not been identified, the bone marrow stromal cell (BMSC) has been identified as a primitive cell type with several attractive properties of a MSC [92]. BMSCs are found in the bone marrow, and when placed in adequate culture conditions in vitro, can differentiate into osteoblasts, fibroblasts, chondrocytes and myoblasts, or when implanted into a host develop into bone, cartilage, fat, muscle, skin and other tissues [92]. BMSCs are attractive for bone tissue engineering because they are able to be seeded into a porous scaffold, proliferate, differentiate into osteoblasts, and enhance bone tissue development in vivo [15, 33, 34, 93, 94]. BMSCs represent one of the most accessible sources of osteoprogenitor cells for therapeutic use [95]. The ease with which they are harvested (a simple marrow aspirate), and the simplicity of the procedures required for their culture and expansion in vitro may make them ideal candidates for bone tissue regeneration [95].

Osteoblastic differentiation in vitro is characterized by three principal periods in cellular activity: proliferation, extracellular matrix maturation, and matrix mineralization (Figure 5) [96]. Proliferation is marked by an exponential increase in cell number and increase in pro-collagen synthesis [97]. During the extracellular matrix maturation phase, cells express alkaline phosphatase (ALP) activity and type I collagen synthesis [96]. The final stage of osteoblast differentiation is matrix mineralization. This stage is marked by expression of extracellular matrix proteins such as osteopontin (OP) and osteocalcin (OC) with accumulation of mineral [98, 99].

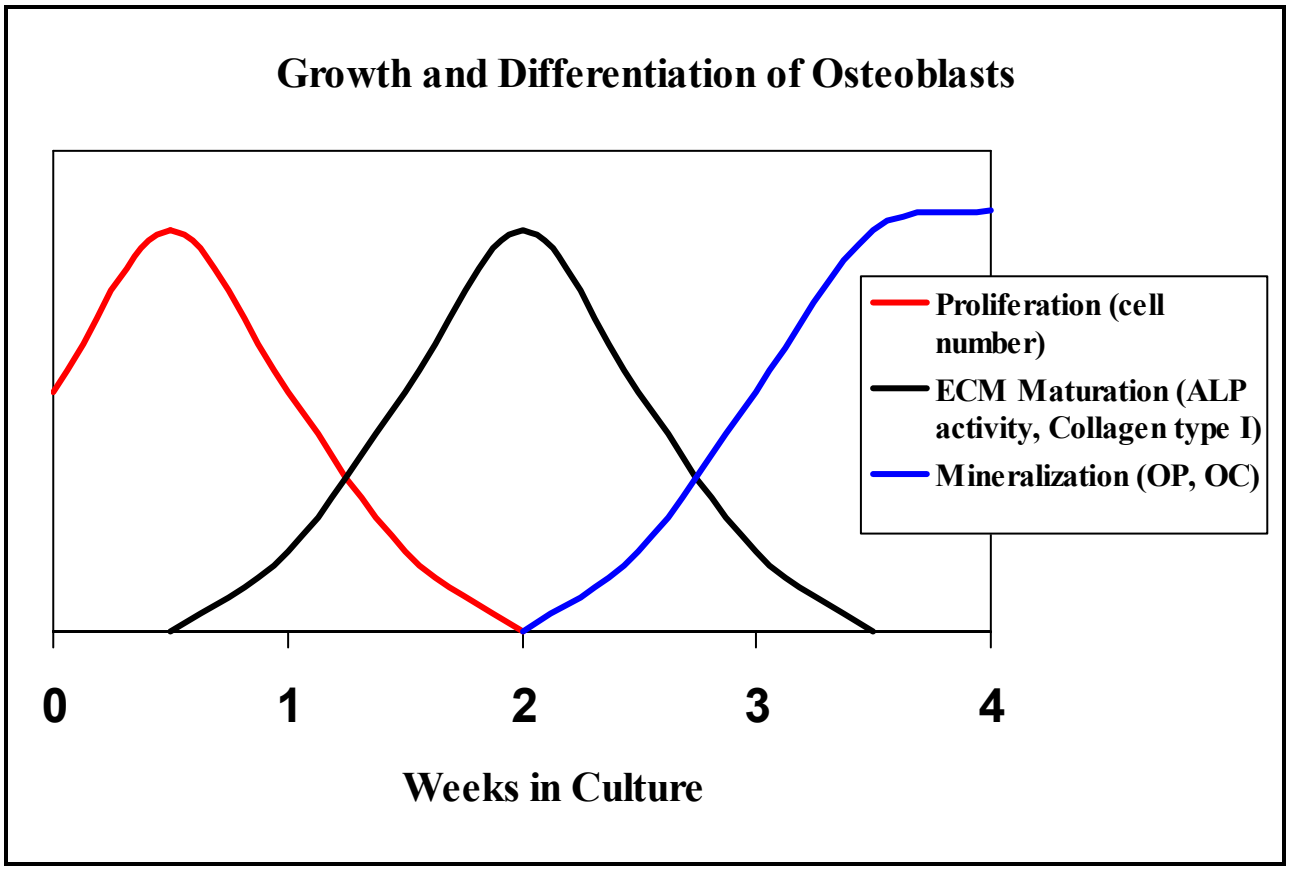

Figure 5: Diagram of three principal periods of osteoblast activity

1.6.2 MC3T3-E1 cell line

The clonally derived murine MC3T3-E1 cell line is one such cell line that expresses markers of the osteoblast phenotype, including alkaline phosphatase activity, type I collagen synthesis, osteopontin expression and matrix mineralization [100]. These cells are useful for in vitro testing of novel materials and culture strategies. The stages of MC3T3-E1 development are similar to those of primary osteoprogenitor cell. During the initial stage of development (days 1-9), MC3T3-E1 cells have been shown to actively replicate, as evidenced by high rates of DNA synthesis, express low alkaline phosphatase activity [101]. After about 9 days, cells undergo growth arrest, express high levels of

alkaline phosphatase activity, and begin processing procollagens to a collagenous extracellular matrix [101]. Mineralization of the extracellular matrix, which begins approximately 16 days after culture, marks the final phase of osteoblast phenotypic development [100]. In order for MC3T3-E1 cells to express phenotypic markers of osteoblastic differentiation in vitro, it has been shown that the culture medium must be supplemented with ascorbic acid (ascorbate) and β-glycerol phosphate [100]. Ascorbate is necessary for cells to convert procollagen to collagen and to consequently incorporate it into the extracellular matrix [101]. β-glycerol phosphate displays synergistic actions with ascorbate to further stimulate collagen accumulation, alkaline phosphatase activity and is necessary for ECM mineralization [101].

1.7 Osteoinductive bone scaffolds

While biomaterials such as poly(α-hydroxy acids), HAP and β-TCP have been shown to be osteoconductive substrates, they are not osteoinductive [9]. These materials could be transformed into osteoinductive scaffolds by incorporating bioactive substances (such as growth factors and bone morphogenetic proteins) into the bulk material or adhering them to the biomaterial surface [9]. Slow degradation of the scaffolds could provide controlled, time-dependent release of incorporated chemical factors, and increase scaffold osteoinductivity [90].

Bone-related growth factors include insulin-like growth factor, fibroblast growth factor, platelet-derived growth factor, and members of the transforming growth factor-β family which increase the mitogenic capacity of the cells [24-26]. For example, transforming growth factor-β1 (TGF-β1) stimulated recruitment and proliferation of

osteoblasts at the sites of bone defects in rabbits, resulting in rapid deposition of bone matrix at defect sites [102, 103]. Platelet-derived growth factor also has been shown to enhance bone deposition at tibial osteotomy sites in rabbits [104].

The bone morphogenetic proteins (BMPs) are members of the TGF-β family and are postulated to increase osteoblastic differentiation [26]. Identified BMPs include BMP 2 - BMP 7 and are currently being investigated for possible clinical use in the repair of bone defects or trauma [26]. The BMPs have received much attention due to their ability to promote bone formation in vitro and in vivo [105-109]. For example, implantation of 0.5 – 115 μg of recombinant human BMP-2 induced ectopic bone formation in rats [110].

Calcium and phosphate ions have also been postulated to be regulators of osteoblastic differentiation [52, 54] and mineralization [53, 55] in vitro, but the mechanisms by which these factors promote osteogenesis remains unknown. Previous in vitro studies have shown that bioactive glass particles [54] and Ca^{+2} and PO_4^{-3} supplements [53] significantly increase osteoblast differentiation. Addition of 1.8 mM calcium and 5 mM inorganic phosphate into cell culture was sufficient to effectively increase in osteoblast mineralization [53] whereas Bioactive glass disks (Bioglass® 45S5) releasing as little as 0.5 mM Ca^{+2} and 0.16 mM PO_4^{-3} into surrounding culture medium enhanced ALP activity in MG63 cells in vitro [54].

1.8 Purpose of study

This project involves both determining MC3T3-E1 osteoblast response to Zr-ACP in vitro and incorporating Zr-ACP into a porous biodegradable PLGA scaffold. Specifically, there were two central aims to the experimental work:

1) Determine osteogenic capability of Zr-ACP on MC3T3-E1 osteoblasts in vitro using HAP as a control

Zr-ACP is promising for use in bone tissue engineered constructs because it is more soluble than hydroxyapatite and allows for controlled release of calcium and phosphate ions; factors that have been postulated to increase osteoblast differentiation and mineralization. The focus of these experiments is to determine the physicochemical properties of Zr-ACP and to measure the cell response to Zr-ACP in vitro using a MC3T3-E1 mouse calvarial-derived osteoprogenitor cell line. Cells were cultured with Zr-ACP or hydroxyapatite, and minerals were added to culture at different stages in cell maturation (days 0, 4 and 11). DNA synthesis, alkaline phosphatase activity, osteopontin expression and collagen synthesis were determined. In addition, calcium and phosphate ion concentrations were measured in cell culture medium from 15 minutes to 2 days after addition of Zr-ACP. Increased osteogenesis is hypothesized to be a result from increased concentrations of calcium and phosphate ions in culture medium after adding Zr-ACP. This study is presented in Chapter 2.

2) Incorporate Zr-ACP into a porous biodegradable PLGA bone scaffold

In these experiments, porous PLGA/Zr-ACP and PLGA/HAP composite foams (5% or 10% (w/v) polymer/solvent with 25 wt% or 50 wt% calcium phosphates) were fabricated using a thermal phase inversion technique. The goals were to form a PLGA/Zr-ACP composite with pore size ranging from 100-350 μm and evenly distribute Zr-ACP into the scaffold while inhibiting Zr-ACP conversion to HAP during processing. X-ray diffractometry was employed to determine Zr-ACP crystallinity after composite fabrication. Pore size, pore distribution, compressive modulus and compressive yield strength of the composites were also determined. This study is presented in Chapter 3.

1.9 References

[1] Yaszemski MJ, Oldham JB, Lu L, Currier BL. Bone engineering. 1st ed. Toronto: Em Squared, 1994.p. 541.

[2] Rose FRAJ, Oreffo ROC. Bone tissue engineering: Hope vs hype. Biochem Biophys Res Comm 2002;292:1-7.

[3] Williams DF. Bone engineering. 1st ed. Toronto: Em Squared, 1999.p. 577.

[4] Patrick CW, Mikos AG, McIntire LV. Frontiers in tissue engineering. 1st ed. Oxford, U.K. ; New York, NY: Pergamon, 1998.p. xvi, 700.

[5] Petite H, Viateau V, Bensaid W, Meunier A, de Pollak C, Bourguignon M, et al. Tissue-engineered bone regeneration. Nat Biotechnol 2000;18:959-963.

[6] Kneser U, Schaefer DJ, Munder B, Klemt C, Andree C, Stark GB. Tissue engineering of bone. Minim Invasiv Ther 2002;11:107-116.

[7] Laurencin CT, Ambrosio AMA, Borden MD, Cooper JA. Tissue engineering: Orthopedic applications. Annu Rev Biomed Eng 1999;1:19-46.

[8] Leong KF, Cheah CM, Chua CK. Solid freeform fabrication of three-dimensional scaffolds for engineering replacement tissues and organs. Biomaterials 2003;24:2363-2378.

[9] Hutmacher DW. Scaffolds in tissue engineering bone and cartilage. Biomaterials 2000;21:2529-2543.

[10] Kuboki Y, Takita H, Kobayashi D, Tsuruga E, Inoue M, Murata M, et al. Bmp-induced osteogenesis on the surface of hydroxyapatite with geometrically feasible and nonfeasible structures: Topology of osteogenesis. J Biomed Mater Res 1998;39:190-199.

[11] Story BJ, Wagner WR, Gaisser DM, Cook SD, Rust-Dawicki AM. In vivo performance of a modified csti dental implant coating. Int J Oral Max Impl 1998;13:749-757.

[12] Freed LE, Vunjak-Novakovic G. Culture of organized cell communities. Adv Drug Deliver Rev 1998;33:15-30.

[13] Karageorgiou V, Kaplan D. Porosity of 3d biomaterial scaffolds and osteogenesis. Biomaterials 2005;26:5474-5491.

[14] Itala AI, Ylanen HO, Ekholm C, Karlsson KH, Aro HT. Pore diameter of more than 100 mu m is not requisite for bone ingrowth in rabbits. J Biomed Mater Res 2001;58:679-683.

[15] Ishaug SL, Crane GM, Miller MJ, Yasko AW, Yaszemski MJ, Mikos AG. Bone formation by three-dimensional stromal osteoblast culture in biodegradable polymer scaffolds. J Biomed Mater Res 1997;36:17-28.

[16] Malekzadeh R, Hollinger JO, Buck D, Adams DF, McAllister BS. Isolation of human osteoblast-like cells and in vitro amplification for tissue engineering. J Periodontol 1998;69:1256-1262.

[17] Mooney DJ, Baldwin DF, Suh NP, Vacanti LP, Langer R. Novel approach to fabricate porous sponges of poly(d,l-lactic-co-glycolic acid) without the use of organic solvents. Biomaterials 1996;17:1417-1422.

[18] Yuan HP, Kurashina K, de Bruijn JD, Li YB, de Groot K, Zhang XD. A preliminary study on osteoinduction of two kinds of calcium phosphate ceramics. Biomaterials 1999;20:1799-1806.

[19] Davies JE. Mechanisms of endosseous integration. International Journal of Prosthodontics 1998;11:391 - 401.

[20] Albrektsson T, Johansson C. Osteoinduction, osteoconduction and osseointegration. Eur Spine J 2001;10:S96-S101.

[21] Gopferich A, Peter SJ, Lucke A, Lu LC, Mikos AG. Modulation of marrow stromal cell function using poly(d,l-lactic acid)-block-poly(ethylene glycol)-monomethyl ether surfaces. J Biomed Mater Res 1999;46:390-398.

[22] Bokhari MA, Akay G, Zhang S, Birch MA. The enhancement of osteoblast growth and differentiation in vitro on a peptide hydrogel--polyhipe polymer hybrid material. Biomaterials 2005;26:5198-5208.

[23] Dames JE, Causton B, Bovell Y, Davy K, Sturt CS. The migration of osteoblasts over substrata of discrete surface charge. Biomaterials 1986;7:231-233.

[24] Finkelman RD, Linkhart TA, Mohan S, Lau KH, Baylink DJ, Bell NH. Vitamin d deficiency causes a selective reduction in deposition of transforming growth factor beta in rat bone: Possible mechanism for impaired osteoinduction. Proc Natl Acad Sci U S A 1991;88:3657-3660.

[25] Mundy GR. Cytokines and growth factors in the regulation of bone remodeling. J Bone Miner Res 1993;8 Suppl 2:S505-510.

[26] Baylink DJ, Finkelman RD, Mohan S. Growth factors to stimulate bone formation. J Bone Miner Res 1993;8 Suppl 2:S565-572.

[27] Reilly DT, Burstein AH, Frankel VH. The elastic modulus for bone. J Biomech 1974;7:271-272.

[28] Rho J-Y, Kuhn-Spearing L, Zioupos P. Mechanical properties and the hierarchical structure of bone. Med Eng & Phys 1998;20:92-102.

[29] Goldstein SA, Matthews LS, Kuhn JL, Hollister SJ. Trabecular bone remodeling: An experimental model. J Biomech 1991;24:135-150.

[30] Langer R, Vacanti JP. Tissue engineering. Science 1993;260:920-926.

[31] Dong J, Kojima H, Uemura T, Kikuchi M, Tateishi T, Tanaka J. In vivo evaluation of a novel porous hydroxyapatite to sustain osteogenesis of transplanted bone marrow-derived osteoblastic cells. J Biomed Mater Res 2001;57:208-216.

[32] Dong JA, Uemura T, Shirasaki Y, Tateishi T. Promotion of bone formation using highly pure porous beta-tcp combined with bone marrow-derived osteoprogenitor cells. Biomaterials 2002;23:4493-4502.

[33] Ishaug-Riley SL, Crane-Kruger GM, Yaszemski MJ, Mikos AG. Three-dimensional culture of rat calvarial osteoblasts in porous biodegradable polymers. Biomaterials 1998;19:1405-1412.

[34] Ishaug SL, Yaszemski MJ, Bizios R, Mikos AG. Osteoblast function on synthetic biodegradable polymers. J Biomed Mater Res 1994;28:1445-1453.

[35] Marra KG, Szem JW, Kumta PN, DiMilla PA, Weiss LE. In vitro analysis of biodegradable polymer blend/hydroxyapatite composites for bone tissue engineering. J Biomed Mater Res 1999;47:324-335.

[36] Glicklis R, Shapiro L, Agbaria R, Merchuk JC, Cohen S. Hepatocyte behavior within three-dimensional porous alginate scaffolds. Biotechnol Bioeng 2000;67:344-353.

[37] Madihally SV, Matthew HWT. Porous chitosan scaffolds for tissue engineering. Biomaterials 1999;20:1133-1142.

[38] Haisch A, Loch A, David J, Pruss A, Hansen R, Sittinger M. Preparation of a pure autologous biodegradable fibrin matrix for tissue engineering. Med Biol Eng Comput 2000;38:686-689.

[39] LeGeros RZ. Properties of osteoconductive biomaterials: Calcium phosphates. Clin Orthop Relat R 2002:81-98.

[40] Radin SR, Ducheyne P. Effect of bioactive ceramic composition and structure on in-vitro behavior .3. Porous versus dense ceramics. J Biomed Mater Res 1994;28:1303-1309.

[41] Hench LL. Bioceramics - from concept to clinic. Am Ceram Soc Bull 1993;72:93-98.

[42] Quarto R, Mastrogiacomo M, Cancedda R, Kutepov SM, Mukhachev V, Lavroukov A, et al. Repair of large bone defects with the use of autologous bone marrow stromal cells. New Engl J Med 2001;344:385-386.

[43] Vacanti CA, Bonassar LJ, Vacanti MP, Shufflebarger J. Replacement of an avulsed phalanx with tissue-engineered bone. New Engl J Med 2001;344:1511-1514.

[44] Grynpas MD, Pilliar RM, Kandel RA, Renlund R, Filiaggi M, Dumitriu M. Porous calcium polyphosphate scaffolds for bone substitute applications in vivo studies. Biomaterials 2002;23:2063-2070.

[45] Yoshikawa T, Ohgushi H, Nakajima H, Yamada E, Ichijima K, Tamai S, et al. In vivo osteogenic durability of cultured bone in porous ceramics - a novel method for autogenous bone graft substitution. Transplantation 2000;69:128-134.

[46] Mendes SC, Sleijster M, van den Muysenberg A, de Bruijn JD, van Blitterswijk CA. A cultured living bone equivalent enhances bone formation when compared to a cell seeding approach. J Mater Sci-Mater M 2002;13:575-581.

[47] Yoshikawa T, Nakajima H, Yamada E, Akahane M, Dohi Y, Ohgushi H, et al. In vivo osteogenic capability of cultured allogeneic bone in porous hydroxyapatite: Immunosuppressive and osteogenic potential of fk506 in vivo. J Bone Miner Res 2000;15:1147-1157.

[48] Maxian SH, Zawadsky JP, Dunn MG. In vitro evaluation of amorphous calcium phosphate and poorly crystallized hydroxyapatite coatings on titanium implants. J Biomed Mater Res 1993;27:111-117.

[49] ter Brugge PJ, Wolke JG, Jansen JA. Effect of calcium phosphate coating composition and crystallinity on the response of osteogenic cells in vitro. Clin Oral Implants Res 2003;14:472-480.

[50] Skrtic D, Antonucci JM, Eanes ED, Brunworth RT. Silica- and zirconia-hybridized amorphous calcium phosphate: Effect on transformation to hydroxyapatite. J Biomed Mater Res 2002;59:597-604.

[51] Skrtic D, Antonucci JM, Eanes ED, Eidelman N. Dental composites based on hybrid and surface-modified amorphous calcium phosphates. Biomaterials 2004;25:1141-1150.

[52] Tenenbaum HC, Heersche JN. Differentiation of osteoblasts and formation of mineralized bone in vitro. Calcif Tissue Int 1982;34:76-79.

[53] Chang YL, Stanford CM, Keller JC. Calcium and phosphate supplementation promotes bone cell mineralization: Implications for hydroxyapatite (ha)-enhanced bone formation. J Biomed Mater Res 2000;52:270-278.

[54] Lossdorfer S, Schwartz Z, Lohmann CH, Greenspan DC, Ranly DM, Boyan BD. Osteoblast response to bioactive glasses in vitro correlates with inorganic phosphate content. Biomaterials 2004;25:2547-2555.

[55] Maeno S, Niki Y, Matsumoto H, Morioka H, Yatabe T, Funayama A, et al. The effect of calcium ion concentration on osteoblast viability, proliferation and differentiation in monolayer and 3d culture. Biomaterials 2005;26:4847-4855.

[56] Lehman WB, Strongwater AB, Tunc D, Kummer F, Atar D, Grant AD, et al. Internal-fixation with biodegradable plate and screws in dogs. J Pediatr Orthop B 1994;3:190-193.

[57] Whang K, Thomas CH, Healy KE, Nuber G. A novel method to fabricate bioabsorbable scaffolds. Polymer 1995;36:837-842.

[58] Zhang M, Haga A, Sekiguchi H, Hirano S. Structure of insect chitin isolated from beetle larva cuticle and silkworm (bombyx mori) pupa exuvia. Int J Biol Macromol 2000;27:99-105.

[59] Tolaimate A, Desbrieres J, Rhazi M, Alagui A. Contribution to the preparation of chitins and chitosans with controlled physico-chemical properties. Polymer 2003;44:7939-7952.

[60] Zhao F, Yin YJ, Lu WW, Leong JC, Zhang WJ, Zhang JY, et al. Preparation and histological evaluation of biomimetic three-dimensional hydroxyapatite/chitosan-gelatin network composite scaffolds. Biomaterials 2002;23:3227-3234.

[61] Deporter DA, Komori N, Howley TP, Shiga A, Ghent A, Hansel P, et al. Reconstituted bovine skin collagen enhances healing of bone wounds in the rat calvaria. Calcified Tissue Int 1988;42:321-325.

[62] Murata M, Huang BZ, Shibata T, Imai S, Nagai N, Arisue M. Bone augmentation by recombinant human bmp-2 and collagen on adult rat parietal bone. Int J Oral Max Surg 1999;28:232-237.

[63] Ueda H, Hong L, Yamamoto M, Shigeno K, Inoue M, Toba T, et al. Use of collagen sponge incorporating transforming growth factor-beta 1 to promote bone repair in skull defects in rabbits. Biomaterials 2002;23:1003-1010.

[64] Salgado AJ, Gomes ME, Chou A, Coutinho OP, Reis RL, Hutmacher DW. Preliminary study on the adhesion and proliferation of human osteoblasts on starch-based scaffolds. Mat Sci Eng C-Bio S 2002;20:27-33.

[65] Elvira C, Mano JF, San Roman J, Reis RL. Starch-based biodegradable hydrogels with potential biomedical applications as drug delivery systems. Biomaterials 2002;23:1955-1966.

[66] Mikos AG, Thorsen AJ, Czerwonka LA, Bao Y, Langer R, Winslow DN, et al. Preparation and characterization of poly(l-lactic acid) foams. Polymer 1994;35:1068-1077.

[67] Thomson RC, Mikos AG, Beahm E, Lemon JC, Satterfield WC, Aufdemorte TB, et al. Guided tissue fabrication from periosteum using preformed biodegradable polymer scaffolds. Biomaterials 1999;20:2007-2018.

[68] Behravesh E, Yasko AW, Engel PS, Mikos AG. Synthetic biodegradable polymers for orthopaedic applications. Clin Orthop Relat R 1999:S118-S129.

[69] Shung AK, Timmer MD, Jo SB, Engel PS, Mikos AG. Kinetics of poly(propylene fumarate) synthesis by step polymerization of diethyl fumarate and propylene glycol using zinc chloride as a catalyst. J Biomat Sci-Polym E 2002;13:95-108.

[70] Hutmacher DW, Schantz T, Zein I, Ng KW, Teoh SH, Tan KC. Mechanical properties and cell cultural response of polycaprolactone scaffolds designed and fabricated via fused deposition modeling. J Biomed Mater Res 2001;55:203-216.

[71] Washburn NR, Simon CG, Tona A, Elgendy HM, Karim A, Amis EJ. Co-extrusion of biocompatible polymers for scaffolds with co-continuous morphology. J Biomed Mater Res 2002;60:20-29.

[72] Schantz JT, Hutmacher DW, Chim H, Ng KW, Lim TC, Teoh SH. Induction of ectopic bone formation by using human periosteal cells in combination with a novel scaffold technology. Cell Transplant 2002;11:125-138.

[73] Schantz JT, Hutmacher DW, Ng KW, Khor HL, Lim TC, Teoh SH. Evaluation of a tissue-engineered membrane-cell construct for guided bone regeneration. Int J Oral Max Impl 2002;17:161-174.

[74] Uhrich KE, Ibim SEM, Larrier DR, Langer R, Laurencin CT. Chemical changes during in vivo degradation of poly(anhydride-imide) matrices. Biomaterials 1998;19:2045-2050.

[75] Suganuma J, Alexander H. Biological response of intramedullary bone to poly-l-lactic acid. J Appl Biomater 1993;4:13-27.

[76] Arnold U, Lindenhayn K, Perka C. In vitro-cultivation of human periosteum derived cells in bioresorbable polymer-tcp-composites. Biomaterials 2002;23:2303-2310.

[77] Calandrelli L, Immirzi B, Malinconico M, Volpe MG, Oliva A, Della Ragione F. Preparation and characterisation of composites based on biodegradable polymers for "in vivo" application. Polymer 2000;41:8027-8033.

[78] Lin ST, Krebs SL, Kadiyala S, Leong KW, Lacourse WC, Kumar B. Development of bioabsorbable glass-fibers. Biomaterials 1994;15:1057-1061.

[79] Mikos AG, Sarakinos G, Leite SM, Vacanti JP, Langer R. Laminated 3-dimensional biodegradable foams for use in tissue engineering. Biomaterials 1993;14:323-330.

[80] Cima LG, Langer R, Vacanti JP. Polymers for tissue and organ-culture. J Bioact Compat Pol 1991;6:232-240.

[81] Mikos AG, Bao Y, Cima LG, Ingber DE, Vacanti JP, Langer R. Preparation of poly(glycolic acid) bonded fiber structures for cell attachment and transplantation. J Biomed Mater Res 1993;27:183-189.

[82] Thomson RC, Yaszemski MJ, Powers JM, Mikos AG. Fabrication of biodegradable polymer scaffolds to engineer trabecular bone. J Biomat Sci-Polym E 1995;7:23-38.

[83] Thomson RC, Yaszemski MJ, Powers JM, Mikos AG. Hydroxyapatite fiber reinforced poly(alpha-hydroxy ester) foams for bone regeneration. Biomaterials 1998;19:1935-1943.

[84] Hsu YY, Gresser JD, Trantolo DJ, Lyons CM, Gangadharam PRJ, Wise DL. Effect of polymer foam morphology and density on kinetics of in vitro controlled release of isoniazid from compressed foam matrices. J Biomed Mater Res 1997;35:107-116.

[85] Dagalakis N, Flink J, Stasikelis P, Burke JF, Yannas IV. Design of an artificial skin .3. Control of pore structure. J Biomed Mater Res 1980;14:511-528.

[86] Doillon CJ, Whyne CF, Brandwein S, Silver FH. Collagen-based wound dressings - control of the pore structure and morphology. J Biomed Mater Res 1986;20:1219-1228.

[87] Schoof H, Bruns L, Fischer A, Heschel I, Rau G. Dendritic ice morphology in unidirectionally solidified collagen suspensions. J Cryst Growth 2000;209:122-129.

[88] Schoof H, Apel J, Heschel I, Rau G. Control of pore structure and size in freeze-dried collagen sponges. J Biomed Mater Res 2001;58:352-357.

[89] Yannas IV, Burke JF. Design of an artificial skin .1. Basic design principles. J Biomed Mater Res 1980;14:65-81.

[90] Hutmacher DW. Scaffold design and fabrication technologies for engineering tissues - state of the art and future perspectives. J Biomat Sci-Polym E 2001;12:107-124.

[91] Aubin J. Bone stem cells. J Cell Biochem Suppl 1998;30:73-82.

[92] Caplan AI. The mesengenic process. Clin Plast Surg 1994;21:429-435.

[93] Crane GM, Ishaug SL, Mikos AG. Bone tissue engineering. Nat Med 1995;1:1322-1324.

[94] Ishaug SL, Payne RG, Yaszemski MJ, Aufdemorte TB, Bizios R, Mikos AG. Osteoblast migration on poly(alpha-hydroxy esters). Biotechnol Bioeng 1996;50:443-451.

[95] Bianco P, Robey PG. Stem cells in tissue engineering. Nature 2001;414:118 - 121.

[96] Lian JB, Stein GS. Concepts of osteoblast growth and differentiation - basis for modulation of bone cell-development and tissue formation. Crit Rev Oral Biol M 1992;3:269-305.

[97] Gerstenfeld LC, Finer MH, Boedtker H. Quantitative-analysis of collagen expression in embryonic chick chondrocytes having different developmental fates. J Biol Chem 1989;264:5112-5120.

[98] Oldberg A, Franzen A, Heinegard D. Cloning and sequence-analysis of rat bone sialoprotein (osteopontin) cdna reveals an arg-gly-asp cell-binding sequence. P Natl Acad Sci USA 1986;83:8819-8823.

[99] Hauschka PV, Wians FH. Osteocalcin-hydroxyapatite interaction in the extracellular organic matrix of bone. Anat Rec 1989;224:180-188.

[100] Sudo H, Kodama HA, Amagai Y, Yamamoto S, Kasai S. Invitro differentiation and calcification in a new clonal osteogenic cell-line derived from newborn mouse calvaria. J Cell Biol 1983;96:191-198.

[101] Quarles LD, Yohay DA, Lever LW, Caton R, Wenstrup RJ. Distinct proliferative and differentiated stages of murine mc3t3-e1 cells in culture - an invitro model of osteoblast development. J Bone Miner Res 1992;7:683-692.

[102] Lind M, Schumacker B, Soballe K, Keller J, Melsen F, Bunger C. Transforming growth factor-beta enhances fracture healing in rabbit tibiae. Acta Orthop Scand 1993;64:553-556.

[103] Beck LS, Amento EP, Xu Y, Deguzman L, Lee WP, Nguyen T, et al. Tgf-beta 1 induces bone closure of skull defects: Temporal dynamics of bone formation in defects exposed to rhtgf-beta 1. J Bone Miner Res 1993;8:753-761.

[104] Nash TJ, Howlett CR, Martin C, Steele J, Johnson KA, Hicklin DJ. Effect of platelet-derived growth factor on tibial osteotomies in rabbits. Bone 1994;15:203-208.

[105] Reddi AH, Cunningham NS. Initiation and promotion of bone differentiation by bone morphogenetic proteins. J Bone Miner Res 1993;8 Suppl 2:S499-502.

[106] Ripamonti U, Ma SS, Cunningham NS, Yeates L, Reddi AH. Reconstruction of the bone--bone marrow organ by osteogenin, a bone morphogenetic protein, and demineralized bone matrix in calvarial defects of adult primates. Plast Reconstr Surg 1993;91:27-36.

[107] Cunningham NS, Paralkar V, Reddi AH. Osteogenin and recombinant bone morphogenetic protein 2b are chemotactic for human monocytes and stimulate transforming growth factor beta 1 mrna expression. Proc Natl Acad Sci U S A 1992;89:11740-11744.

[108] Luyten FP, Cunningham NS, Vukicevic S, Paralkar V, Ripamonti U, Reddi AH. Advances in osteogenin and related bone morphogenetic proteins in bone induction and repair. Acta Orthop Belg 1992;58 Suppl 1:263-267.

[109] Ripamonti U, Ma S, Cunningham NS, Yeates L, Reddi AH. Initiation of bone regeneration in adult baboons by osteogenin, a bone morphogenetic protein. Matrix 1992;12:369-380.

[110] Wang EA, Rosen V, D'Alessandro JS, Bauduy M, Cordes P, Harada T, et al. Recombinant human bone morphogenetic protein induces bone formation. Proc Natl Acad Sci U S A 1990;87:2220-2224.

[111] Salgado AJ, Coutinho OP, Reis RL. Novel starch-based scaffolds for bone tissue engineering: Cytotoxicity, cell culture, and protein expression. Tissue Eng 2004;10:465-474.

Chapter 2: Osteoblast Response to Zirconia-Hybridized Pyrophosphate Stabilized Amorphous Calcium Phosphate

Bryce M. Whited[1], Aaron S. Goldstein[1,2], Drago Skrtic[4], Brian J. Love[1,3]

[1]School of Biomedical Engineering and Sciences, Departments of
[2]Chemical and [3]Materials Science and Engineering
Virginia Polytechnic Institute and State University Blacksburg, VA 24061-0211
[4]American Dental Association Foundation, Paffenbarger Research Center, National Institute of Standards and Technology, 100 Bureau Drive Stop 8546, Gaithersburg, MD 20899

2.1 Abstract

Calcium phosphate bioceramics, such as hydroxyapatite, have long been used as bone substitutes due to their proven biocompatibility and bone binding properties in vivo. Recently, a zirconia-hybridized pyrophosphate stabilized amorphous calcium phosphate (Zr-ACP) has been synthesized to increase rates of remineralization for craniofacial applications. Zr-ACP is promising for use in bone tissue scaffolds because it is more soluble than hydroxyapatite and allows for controlled release of calcium and phosphate ions. These ions have recently been postulated to increase osteoblast differentiation and mineralization in vitro. The focus of this work is to elucidate the physicochemical properties of Zr-ACP and to measure cell response to Zr-ACP in vitro using a MC3T3-E1 mouse calvarial-derived osteoprogenitor cell line. Cells were cultured in osteogenic medium with and without Zr-ACP or hydroxyapatite, and minerals were added to culture at different stages in cell maturation (days 0, 4 and 11). DNA synthesis, alkaline phosphatase activity, osteopontin synthesis and collagen synthesis were determined. Culture in the presence of Zr-ACP showed significant increase in cell proliferation,

alkaline phosphatase activity and osteopontin expression, whereas collagen synthesis was unaffected. In addition, calcium and phosphate ion concentrations were measured in cell culture medium from 15 minutes to 2 days after the addition of Zr-ACP. Increased osteogenesis is hypothesized to result from increased concentrations of calcium and phosphate ions released into culture medium with the addition of Zr-ACP. These results demonstrate that Zr-ACP promotes osteogenesis in MC3T3-E1 osteoblasts.

2.2 Introduction

Calcium phosphate ceramics have long been the subject of intensive investigation for repairing osseous defects [1]. This group of biomaterials includes hydroxyapatite (HAP), α-tricalcium phosphate and β-tricalcium phosphate which have been used to form porous bone scaffolds to aid bone regeneration in bone defects. These ceramics exhibit excellent biocompatibility, osteoconductivity and bind directly to bone tissues in vivo [2-4]. While porous calcium phosphate scaffolds eventually serve to repair osseous defects, there is no evidence that these calcium phosphate scaffolds are osteoinductive [5, 6]. An osteoinductive material would allow for better cell differentiation and would aid in normal osteoblastic functions (adhesion, proliferation, mineralization, etc.) as compared to a non-osteoinductive material [6]. There is therefore a need to find a suitable osteoinductive material for use as bone scaffolds to aid in bone regeneration when implanted into bone defects.

Calcium and phosphate ions have been postulated to be regulators of osteoblastic differentiation [7, 8] and mineralization [9, 10] in vitro, but the mechanisms by which these factors promote osteogenesis remains unknown. A ceramic scaffold material able

to release controlled amounts of these ions may increase the osteoinductivity of the scaffold and promote bone tissue regeneration. Recently, amorphous calcium phosphate has been stabilized by ions (pyrophosphate, $P_2O_7^{-4}$) and hybridized with zirconium (Zr-ACP) that retard its conversion to HAP while maintaining substantial release of Ca^{+2} and PO_4^{-3} ions in aqueous environments over long periods of time [11, 12]. Our hypothesis is that Zr-ACP, when incorporated into a bone scaffold, can act as a vehicle to deliver ions of interest to osteoblasts and subsequently enhance osteoblastic differentiation, extracellular matrix maturation and eventual bone tissue regeneration in vivo.

Osteoblasts are useful for studying bone metabolism and evaluation of osteoconductive and osteoinductive properties of biomaterials. We chose to employ a MC3T3-E1 mouse calvaria-derived osteoprogenitor cell line because of their proven differentiation in vitro, exhibiting developmental stage-specific gene expression as seen in vivo [13]. Osteoblast differentiation is characterized by three principal periods of cellular activity: proliferation, extracellular matrix maturation and matrix mineralization [14]. Proliferation is the first period and is marked by an exponential increase in cell number and the accumulation of procollagen [15]. The matrix maturation phase is characterized by an increase of alkaline phosphatase (ALP) activity and collagen synthesis [14]. The final stage of osteoblast differentiation is matrix mineralization. This stage is marked by expression of extracellular matrix proteins such osteopontin and osteocalcin and accumulation of mineral [16, 17].

The aim of this study is to evaluate osteoblast cell activity when exposed to Zr-ACP and to analyze the physicochemical modifications of the material in cell culture conditions. Change in pH and ion concentration (Ca^{+2} and PO_4^{-3}) in cell culture medium

were measured to determine changes in culture conditions. Five mg/ml Zr-ACP, HAP or no mineral (control) were added at days 0, 4, or 11 to characterize their effects on the different stages osteoblastic differentiation. Cell number and ALP activity were determined at days 3, 5, 7, 10, 12, 14 and osteopontin and collagen synthesis were measured at day 14.

2.3 Materials and methods

2.3.1 Zr-ACP synthesis and characterization

Calcium nitrate tetrahydrate [$Ca(NO_3)_2x4H_2O$], dibasic sodium phosphate [Na_2HPO_4], sodium pyrophosphate [$Na_4P_2O_7x10H_2O$] and sodium hydroxide [NaOH] were purchased from Sigma-Aldrich (St. Louis, MO). Ammonium hydroxide and acetone were purchased from Fisher (Fairlawn, NJ). Zirconyl chloride [$ZrOCl_2$] was purchased from GFS Chemicals (Columbus, OH).

Zr-ACP and HAP were prepared at the American Dental Association Paffenbarger Research Center according to the method of Skrtic et al. [11]. Briefly, for Zr-ACP, a 1.06M solution of a $Ca(NO_3)_2x4H_2O$ was prepared using CO_2-free water (N_2 closed system) (designated as solution 1). Forty ml of a 0.25 M $ZrOCl_2$ solution was prepared and designated as solution 2. A 1.16M Na_2HPO_4 solution including 0.024M $Na_4P_2O_7x10H_2O$ was made using CO_2-free water (mechanically stirred at 400 rpm) and 67 ml of a 1M NaOH solution was added under N_2 in a covered beaker where pH of 8.5 to 9 was measured (designated as solution 3). Solutions 1 and 2 were added simultaneously to solution 3 under N_2 and mechanically stirred at 400-500 rpm. Precipitation of the Zr-ACP was instantaneous. The solution was allowed to stabilize for

5 minutes, where after precipitates were filtered and washed twice with cold ammoniated water (2% ammonia) and then washed with cold acetone. Zr-ACP was then frozen in a -50^{o}C freezer for one hour and transferred to a VirTis bench top freeze dry system (SP Industries, Inc., Warminster, PA) for 48 hours at a temperature of -70^{o}C and pressure of 5 mTorr.

The crystallinity of the lyophilized solids was verified by powder X-ray diffractometry (XRD). The XRD profiles were recorded in the range of 15^{o} to 70^{o} with CuKα X-ray source (λ=1.54Å) using a XDS 2000 (Scintac Inc., USA) operated at 40kV and 40mA. The samples were step scanned in intervals of 0.020^{o} at a scanning speed of 2.000^{o}/min. Further characterization of the materials in terms of crystallinity, surface morphology, Ca/PO_4 molar ratios and dissolution/transformation of Zr-ACP is extensively documented in the literature [11, 12].

2.3.2 Physicochemical evaluation of calcium phosphates in growth medium

Change in pH and concentrations of Ca^{+2} and PO_4^{-3} ions were determined after addition of calcium phosphates to growth medium (minimum essential medium alpha modification; Invitrogen, Gaithersburg, MD) with 10% Fetal Bovine Serum (Gemini Bioproducts, Calabasas, CA) and 1% antibiotic/antimycotic (penicillin, streptomycin, neomycin, fungizone; Invitrogen)). Growth medium was incubated in a 37°C, 5% CO_2, 95% relative humidity environment one day prior to experimentation. Ten mg Zr-ACP, HAP or no mineral was added to 2ml of growth medium at time 0. Aliquots of growth medium from each sample was removed at 15 min, 30 min, 1 hr, 12 hrs, 24 hrs and 48 hrs, pH was measured, centrifuged for 10 min at 10,000 rpm to remove any insoluble

species, and then stored in 1.5ml microcentrifuge tubes. Ion chromatography determined concentrations of Ca^{+2} and PO_4^{-3} using a Dionex DX-120 (Dionex, Sunnyvale, CA) ion chromatigraph. Calcium concentration was determined by using a AS9-HC (Dionex) cation column and PO_4^{-3} concentration using a CS12-A (Dionex) anion column.

2.3.3 Cell culture

Cell studies were performed with a MC3T3-E1 cell line donated by Dr. A.J. García (Department of Mechanical Engineering, Georgia Institute of Technology, Atlanta, GA). Cells were maintained with growth medium in a 37°C, 5% CO_2, 95% relative humidity environment for 14 days and used at passages below 20.

For studies, cells were lifted with trypsin/EDTA (Gibco BRL), seeded in 12-well culture plates (Corning, Corning, NY) at 50,000 cells/well with 2ml growth medium and allowed to attach overnight. The following day, designated as day 0, growth medium was replaced with differentiation medium (growth medium supplemented with 37.5μg/ml L-ascorbate-2-phosphate (Sigma-Aldrich, St. Louis, MO)). Medium was replaced on days 3, 7 and 10. To determine the impact of Zr-ACP and HAP on the stages of cell development, material was added directly to cell culture at a concentration of 5mg/ml at days 0, 4 and 11. Cell number and alkaline phosphatase (ALP) activity were measured at days 3, 7, 10 and 14 for material addition at day 0, at days 5, 7 and 14 for material addition at day 4, and at days 12 and 14 for material addition at day 11. Osteopontin and collagen synthesis were measured at day 14 for all conditions.

2.3.4 Measurement of cell number

Fluorometric analysis of DNA content was used to determine the total number of cells for each condition as described previously [18]. Briefly, one 0.5-mL aliquot of 10 mM EDTA (pH 12.3) was pipetted into each well, cell layers were scraped and collected into 1.5-mL microcentrifuge tubes. Another 0.5-mL aliquot of 10 mM EDTA was then added to the wells and then pipetted into the same tubes. DNA standards were made by adding 0, 1, 2, 4, 6, 7, 8 or 10 μg DNA standard to 10mM EDTA (pH 12.3) to a final volume of 1 ml. Here, a 50 μg/mL DNA solution corresponds to an absorbance of 1.00 through a path of 1 cm at 260 nm. A volume of 0.2 ml of 1 M KH_2PO_4 was added to each sample in order to neutralize pH after sonication. Measurements were made in duplicate with a DyNAQuant 200 (Hoefer, San Francisco, CA). A calibration curve showing a linear relationship between fluorescence and the concentrations of the DNA standards was used to ultimately determine DNA concentrations. A conversion factor of 9.1 pg DNA/cell (determined experimentally for MC3T3-E1 cells) was used to determine cell number.

2.3.5 Alkaline Phosphatase Activity

The hydrolysis of *p*-nitrophenyl phosphate was used to assay ALP activity, an early indicator of osteoblastic phenotype [19]. Briefly, a 0.5-mL aliquot of a 1% solution of protease inhibitors (2.0 μg/mL aproptinin, 2.0 μg/mL leupeptin, 1.0 μg/mL pepstatin (Calbiochem, La Jolla, CA) in TG solution (50 mM Tris, 100 mM glycine, pH 10.5; Sigma-Aldrich) in TGT solution (50 mM Tris, 100 mM glycine, and 0.1% Triton X-100, pH 10.5; Sigma Aldrich) was added to each well, cell layers were scraped and collected

into 1.5-mL microcentrifuge tubes. Another 0.5-mL aliquot of cell lysate was then added to the wells and then pipetted into the same tubes. For each sample, a 200 µL volume was combined with 1 mL of Alkaline Phosphatase (ALP) reagent (BioTron Diagnostics, Inc., Hemet, CA) at 30°C. A Genesis 5 spectrophotometer (Spectronic Instruments, Rochester, NY) was used to measure absorbance at 405 nm at zero minutes and at one minute intervals up to three minutes. Activity was calculated using the slope of absorbance versus time and normalized by cell number.

2.3.6 Osteopontin Synthesis

Osteopontin, an extracellular matrix protein synthesized during the mineralization stage, was characterized by western blot analysis as described previously [20]. Equal volumes of cell lysate (3.5 µl/lane) were analyzed for each sample. Briefly, cell layers were washed twice with PBS, mechanically scraped, and lysed with 1X Laemmli buffer (950 µL Laemmli stock solution (Biorad, Hercules, CA), 50 µL β-mercaptoethanol (Fisher), and 1 mL PBS). Samples were denatured at 90^{o}C for 1.5 minutes using a bench-top dry bath incubater (Fisher Scientific) and immediately placed on ice. Protein samples were separated for 1.25 hours at 125V with a Bio-Rad power pac 200 electrophoresis power supply (Bio-Rad Laboratories, Hercules, CA) using a 7.5% SDS-PAGE running gel. Proteins were transferred to an Immune-blot polyvinylidene diflouride membrane (Bio-Rad Laboratories, Hercules, CA) for 1.5 hours at 100 V. Membranes were then blocked at room temperature for one hour in TBS-T (4.44g/L Tris-HCl, 2.65g/L tris base, 8.766g/L NaCl, 1mL/L Tween 20 in deionized) on a clinical rotator. Rabbit anti-mouse osteopontin primary antibodies (Assay Designs, Ann Arbor, MI) were used as 1/500

dilution in TBS-T (5% dry milk in TBS-T) and incubated on a clinical rotator overnight at 4°C. Next, a horseradish peroxidase (HRP) conjugated goat anti-rabbit antibody was used as a 1/15000 dilution (Zymed Laboratories, San Francisco, CA) and incubated at room temperature for one hour. Detection of the protein bands were carried out by using an enhanced chemiluminescent substrate for detection of HRP (Super Signal West Pico Chemiluminescent substrate, Pierce Co., Rockford, IL), and were visualized by chemiluminescence using Kodak X-Omat film.

Glyceraldehyde-3-phosphate dehydrogenase (G3PDH; Santa Cruz Biotechnology Santa Cruz, CA) HRP conjugated antibody was used as an internal control for western blots. After protein detection for the western blots were complete, membranes were stripped with stripping buffer (2% sodium dodecyl sulfate, 100 mM beta-mercaptoethanol, 50 mM Tris, pH 6.8, Sigma Aldrich) and agitated for 20 minutes at 50°C. Membranes were then incubated for 1 hour in a 1/500 dilution of G3PDH antibody, detected using the Super Signal West Pico Chemiluminescent substrate and visualized with Kodak X-Omat film.

2.3.7 Collagen Synthesis

Collagen synthesis was determined by the incorporation of radiolabeled proline (^{3}H-proline) [18]. Forty-eight hours prior to sample collection, 6 µl of 1 µCi/µl ^{3}H-proline stock solution (ICN, Irvine, CA) was added to the culture medium. After incubating the wells in a 5% CO_2, 37°C, 95% relative humidity incubator for 48 hours, the medium was removed and the wells were rinsed twice with 2 ml PBS. A 1 ml volume of nonspecific digestion solution (1 mg/ml pepsin (Sigma, St. Louis, MO) in 1 M

acetic acid (Fisher, Pittsburgh, PA)) was added to each well and incubated for 4 hours at room temperature. Next, the wells were rigorously scraped and two 200 µl aliquots were transferred to individual 1.5 ml microcentrifuge tubes. For each subsample, 100 µl of 0.6 M *N*-2-hydroxyethylpiperazine *N'*-2-ethane sulfuric acid (HEPES, pH 7.0; Sigma) and 200 µl of a collagen-specific digestion solution (6.25 mM n-ethyl-multimode (Sigma), 1.25 mM $CaCl_2 \cdot 2H_2O$ (Sigma) and 125 µg/ml collagenase (Sigma #C0773) in 0.02 N HCl (Fisher)) was added. The tubes were incubated in a 37°C water bath for 90 minutes. The digestion was then quenched by adding a 500 µl aliquot of 10% trichloroacetic acid and 0.5% tannic acid (10% TCA/0.5% TA).

The tubes were mixed, chilled on ice for approximately 10 minutes, and centrifuged at 2,000 x g for 5 minutes. A 900 µl aliquot of each supernatant was added to individual 5 ml scintillation vials. The pellets were resuspended in 500 µl of 5% TCA/0.25 %TA solution, chilled on ice, and centrifuged again at 2000 x g for 5 minutes. Each 500 µl aliquot of this supernatant was added to the same scintillation vials as before, yielding a total of 1.4 ml supernatant per subsample. These vials were designated as containing the collagenase-digestible protein fraction. The pellets were resuspended with 1.3 ml of 5% TCA/ 0.25% TA, and the entire tube volumes were transferred to separate scintillation vials. These vials were designated as containing the non-collagenase-digestible protein fraction. Four ml of immulsion type liquid scintillant was added to each vial, and counts were measured using a Tricarb 2100TR beta-counter (Packard, Palo Alto, CA). Counts for collagenase-digestible and non-digestible fractions were normalized by the mean cell densities. The percent collagenous protein (%CP) for each sample was calculated using the following formula [21]:

$$\%CP = \left[\frac{CP}{(CP + 5.2 \times NCP)} \right] \times 100\%$$

The number 5.2 in this equation accounts for the relative abundance of proline in collagen.

2.3.8 Statistical Analysis

Values are presented as mean ± standard deviation unless otherwise noted. Statistical analysis was performed using Origin® 6.1 (OriginLab, Northampton, MA). A one-way analysis of variance (ANOVA) procedure with a significance level (α) of 0.05 was used to determine significant differences between groups.

2.4 Results

2.4.1 Calcium phosphate interaction with culture medium

XRD was used to characterize the crystallinity of Zr-ACP and HAP. XRD patterns for Zr-ACP lack discrete diffraction peaks, indicating an amorphous structure (Figure 1a). In contrast, HAP shows discrete diffraction peaks indicative of a crystalline structure (Figure 1b). The amorphous structure of Zr-ACP has been shown to increase solubility of Zr-ACP and subsequently release more Ca^{+2} and PO_4^{-3} ions in phosphate buffered saline (pH: 7.4) than HAP [11]. To determine the dynamic effects of Zr-ACP and HAP in tissue culture, minerals were added to growth medium and analyzed at discrete points in time. Ion chromatography confirmed transient increases of Ca^{+2} and PO_4^{-3} in cell culture medium for Zr-ACP as compared to HAP (Figures 2a, b). For Zr-ACP, phosphate concentrations increased from 0.19 ± 0.04 mM to 0.58 ± 0.03 mM after 15 min and then decreased to 0.29 ± 0.02 mM after 2 days. Likewise, calcium

concentrations increased from 0.85 ± 0.03 mM to 1.58 ± 0.6 mM after 15 min and then decreased to 0.30 ± 0.09 mM after 2 days. It appears that a calcium phosphate mineral was precipitated out of solution for medium containing HAP, as calcium and phosphate ions decreased over time (Figures 2a, b).

The growth medium containing HAP remained relatively constant throughout testing, ranging from a pH of 7.30 ± 0.01 to 7.35 ± 0.01 and closely tracked the pH of medium with out mineral (Figure 3). In constrast, Zr-ACP transformation caused a slight rise in pH of the growth medium from 7.35 ± 0.06 to 7.53 ± 0.06 after immersion for 15 minutes and then slowly decreased back to a pH of 7.35 ± 0.01 after 48 hours (Figure 3).

2.4.2 Cell Number

To determine the effect of minerals on cell proliferation, cell number was measured at days 3, 5, 7, 10, 12, and 14. Quantification of DNA indicated that cell number increased rapidly the first three days of culture for conditions with mineral added at day 0 from an initial seeding density of 50,000 cells per well (Figure 4). Differences in cell numbers were not statistically significant at days 3 and 7 for tests in which materials were added at day 0. Exposure to Zr-ACP for 10 and 14 days resulted in significantly higher cells per well ($P<0.05$) as compared to the control. A decrease in cell number was found when HAP was added to cell culture at days 4 and 11 (Figure 5).

2.4.3 Alkaline Phosphatase Activity

Cells were assayed for alkaline phosphatase activity at days 3, 7, 10 and 14 after addition of materials at day 0 to determine if the cells were differentiating towards the

osteoblast phenotype. Cellular ALP activity was also measured shortly after material exposure to determine transient effects. Assays were completed at days 5, 7 and 14 for cells exposed to materials at day 4, and assayed at days 12 and 14 for cells exposed to materials at day 11. When materials were added at day 0, no effect on ALP activity was observed at days 3, 7, 10 and 14 (data not shown). However, when added at days 4 and 11, transient increases in ALP activity were observed at days 5 and 12 but diminished by days 7 and 14 respectively (Figures 6a, 6b). These results indicate that addition of Zr-ACP to cell culture significantly increased ALP activity transiently after addition of the material.

2.4.4 Osteopontin Expression

At day 14, cells were assayed for osteopontin: a protein expressed by osteoblasts during cell proliferation and matrix mineralization. Groups included cultures exposed to materials at days 0, 4 and 11. Osteopontin band densities were normalized by using G3PDH as an internal control. Western blots indicated a 4 fold decrease in osteopontin expression for cells exposed to HAP at day 0 (Figure 7a). In contrast, a significant 2-fold increase ($P<0.05$) in osteopontin expression was measured when both Zr-ACP and HAP were added at days 4 and 11 as compared to the control (Figure 7b).

2.4.5 Collagen Synthesis

Incorporation of ^{3}H-proline into the collagenase-digestible protein fraction revealed no significant changes in collagenous protein as a percentage of total protein synthesized between conditions (Figure 8a). A modest, but statistically insignificant,

increase in collagen synthesis rate per cell was measured for conditions with mineral (Figure 8b). Together they indicated that collagen synthesis was not significantly affected by treatments.

2.5 Discussion

In addition to biocompatibility, the three most important features of a bone implant are: integration, vascular infiltration and osteogenesis. These desirable effects are obtained by stimulation of osteoblastic activity [22]. Previous studies have revealed that hydroxyapatite and other forms of calcium phosphates are osteoconductive and promote osteoblast function [23-26]. This study indicates that Zr-ACP increases osteoblast function by affecting proliferation, ALP activity, and ECM production of MC3T3-E1 cells to a greater extent than HAP in vitro.

The initial phase of osteoblast development is characterized by active replication of undifferentiated cells [13]. During the first several days, subconfluent cultures display rapid increases in cell number and high rates of DNA synthesis. Rapid cell proliferation was seen for all conditions where materials were added to culture at day 0. Cell numbers increased from 5×10^5 cells/well at day 0 to about 3×10^6 cells/well at day 3 for all conditions (Figure 4). This rapid proliferation was followed by a more moderate increase in cell number for all conditions to day 14. Increased cell number in the presence of Zr-ACP at days 10 and 14 indicate that MC3T3-E1 cells responded to this material by stimulating the proliferative activity (Figure 4). A decrease in cell number was seen for cells exposed to HAP at days 4 and 11 (Figure 5), although HAP had no effect on alkaline phosphatase activity. HAP is considered to be a well tolerated material,

however, in vitro studies have shown cell death and inhibition of proliferation. Toxic effects appear in vitro with HAP particle sizes less than about 5μm [27], and are thought to be related the phagocytic activity of the osteoblasts and inhibition of DNA synthesis [28]. HAP particles used in this study ranged in size from 1 – 10 μm [11] and therefore could have increased the phagocytic activity of these cells when added at later times to cell culture.

The initial period of cell growth is followed by the matrix maturation phase: an intermediate phase characterized by diminished cell growth and expression of the bone cell phenotype. The decrease in replication is coupled to expression of ALP activity, one marker of mature osteoblast function [14]. ALP activity was transiently increased almost 2.5 times over the control at day 5, and almost 1.5 times the control at day 12 for cells exposed to Zr-ACP (Figures 5a, b). These increases in ALP activity coincided with the transient increase in Ca^{+2} and PO_4^{-3} concentrations in cell culture medium. Previous in vitro studies have shown that inclusion of bioactive glass particles [7] and Ca^{+2} and PO_4^{-3} supplements [9] significantly increase osteoblast differentiation. Addition of 1.8 mM calcium and 5 mM inorganic phosphate was sufficient to effectively increase in osteoblast mineralization [9] whereas Bioactive glass disks (Bioglass® 45S5) releasing as little as 0.5 mM Ca^{+2} and 0.16 mM PO_4^{-3} into surrounding culture medium enhanced ALP activity in MG63 cells [7]. Our results show that dissolution of Zr-ACP supplemented culture medium with 0.58 mM PO_4^{-3} and 1.58 mM Ca^{+2} and upregulated ALP activity of the osteoblasts.

β-glycerol phosphate was excluded from the cell culture medium for these experiments. This compound is a substrate for alkaline phosphatase and increases the

local phosphate concentration whenever the enzyme is present. It has previously been shown that β-glycerol phosphate magnifies the effects of ascorbate-2-phosphate on the increase of alkaline phosphatase activity on MC3T3-E1 osteoblasts in vitro [13]. The reason for its exclusion from cell culture medium with these experiments was to evaluate the effects of increased phosphate on cells evolved directly from the Zr-ACP.

Osteopontin and collagen were assayed at day 14 to determine effects of Zr-ACP and HAP on extracellular matrix maturation. Osteopontin is a phosphoprotein that is expressed both during cell proliferation and matrix mineralization of osteoblasts [13, 14] and has both HAP and cell binding domains. A number of in vitro studies have revealed that osteopontin binds to the calcium phosphate crystals in mineralized tissue and inhibits crystal growth through its abundant aspirate and phosphorylated serine residues [29-31]. Our findings demonstrate that Zr-ACP and HAP stimulate osteopontin at both the proliferative (days 1-9) and matrix maturation (days 9-16) stages of osteoblast development [13]. These findings are consistent with previous studies using various calcium phosphates [32, 33]. There were no significant differences between conditions with Zr-ACP and HAP when added at days 4 and 11, although both were significantly greater than the control. One explanation for an increase in osteopontin is that the high levels of calcium phosphates that were in contact with the cells could have resembled a highly mineralized matrix, and therefore upregulated osteopontin expression relative to the control [29].

Collagen is the principal structural component of the bone extracellular matrix and binds Ca^{+2} to hydroxyapatite [34]. Collagen is initially synthesized during the proliferation period when their mRNA levels are the highest, however, synthesis and

increased accumulation of collagen continues throughout the culture period and is processed more rapidly and accumulates more efficiently during the matrix maturation stage [14]. MC3T3-E1 collagen synthesis was not significantly affected by the presence of either Zr-ACP or HAP in cell culture for these experiments. In the isolated osteoblast culture system, it has been demonstrated that alkalosis of culture medium to pH 7.6 causes an increase in collagen synthesis [35]. Even though a small increase in pH was measured for medium containing Zr-ACP (pH: 7.53), a subsequent increase in collagen synthesis was not found.

2.6 Conclusions

The results of this study demonstrate that Zr-ACP significantly increases proliferation, alkaline phosphatase activity and osteopontin expression in MC3T3-E1 osteoblasts in vitro. The enhanced dissolution capacity of Zr-ACP over HAP may imply that it is able to enhance new bone formation by supplying calcium and phosphate ions under culture conditions, and therefore increase phenotypic expressions of osteoprogenitor cell lines. The osteogenic nature of Zr-ACP shows great promise for incorporation into bone substitutes with the potential to regulate bone regeneration and osteoblast activity adjacent to the biomaterial.

2.7 References

[1] Bohner M. Calcium orthophosphates in medicine: from ceramics to calcium phosphate cements. Injury 2000;31 Suppl 4:37-47.

[2] Eggli PS, Muller W, Schenk RK. Porous hydroxyapatite and tricalcium phosphate cylinders with two different pore size ranges implanted in the cancellous bone of rabbits. A comparative histomorphometric and histologic study of bony ingrowth and implant substitution. Clin Orthop Relat Res 1988:127-138.

[3] Saffar JL, Colombier ML, Detienville R. Bone formation in tricalcium phosphate-filled periodontal intrabony lesions. Histological observations in humans. J Periodontol 1990;61:209-216.

[4] Schmitz JP, Hollinger JO, Milam SB. Reconstruction of bone using calcium phosphate bone cements: a critical review. J Oral Maxillofac Surg 1999;57:1122-1126.

[5] Goshima J, Goldberg VM, Caplan AI. Osteogenic potential of culture-expanded rat marrow cells as assayed in vivo with porous calcium phosphate ceramic. Biomaterials 1991;12:253-258.

[6] Harris CT, Cooper LF. Comparison of bone graft matrices for human mesenchymal stem cell-directed osteogenesis. J Biomed Mater Res A 2004;68:747-755.

[7] Lossdorfer S, Schwartz Z, Lohmann CH, Greenspan DC, Ranly DM, Boyan BD. Osteoblast response to bioactive glasses in vitro correlates with inorganic phosphate content. Biomaterials 2004;25:2547-2555.

[8] Tenenbaum HC, Heersche JN. Differentiation of osteoblasts and formation of mineralized bone in vitro. Calcif Tissue Int 1982;34:76-79.

[9] Chang YL, Stanford CM, Keller JC. Calcium and phosphate supplementation promotes bone cell mineralization: implications for hydroxyapatite (HA)-enhanced bone formation. J Biomed Mater Res 2000;52:270-278.

[10] Maeno S, Niki Y, Matsumoto H, Morioka H, Yatabe T, Funayama A, et al. The effect of calcium ion concentration on osteoblast viability, proliferation and differentiation in monolayer and 3D culture. Biomaterials 2005;26:4847-4855.

[11] Skrtic D, Antonucci JM, Eanes ED, Brunworth RT. Silica- and zirconia-hybridized amorphous calcium phosphate: effect on transformation to hydroxyapatite. J Biomed Mater Res 2002;59:597-604.

[12] Skrtic D, Antonucci JM, Eanes ED, Eidelman N. Dental composites based on hybrid and surface-modified amorphous calcium phosphates. Biomaterials 2004;25:1141-1150.

[13] Quarles LD, Yohay DA, Lever LW, Caton R, Wenstrup RJ. Distinct Proliferative and Differentiated Stages of Murine Mc3t3-E1 Cells in Culture - an Invitro Model of Osteoblast Development. J Bone Miner Res 1992;7:683-692.

[14] Lian JB, Stein GS. Concepts of Osteoblast Growth and Differentiation - Basis for Modulation of Bone Cell-Development and Tissue Formation. Crit Rev Oral Biol M 1992;3:269-305.

[15] Gerstenfeld LC, Finer MH, Boedtker H. Quantitative-Analysis of Collagen Expression in Embryonic Chick Chondrocytes Having Different Developmental Fates. J Biol Chem 1989;264:5112-5120.

[16] Oldberg A, Franzen A, Heinegard D. Cloning and Sequence-Analysis of Rat Bone Sialoprotein (Osteopontin) Cdna Reveals an Arg-Gly-Asp Cell-Binding Sequence. P Natl Acad Sci USA 1986;83:8819-8823.

[17] Hauschka PV, Wians FH. Osteocalcin-Hydroxyapatite Interaction in the Extracellular Organic Matrix of Bone. Anat Rec 1989;224:180-188.

[18] Porter RM, Huckle WR, Goldstein AS. Effect of dexamethasone withdrawal on osteoblastic differentiation of bone marrow stromal cells. J Cell Biochem 2003;90:13-22.

[19] Goldstein AS, Juarez TM, Helmke CD, Gustin MC, Mikos AG. Effect of convection on osteoblastic cell growth and function in biodegradable polymer foam scaffolds. Biomaterials 2001;22:1279-1288.

[20] Kreke MR, Huckle WR, Goldstein AS. Fluid Flow Stimulates Expression of Osteopontin and Bone Sialoprotein by Bone Marrow Stromal Cells in a Temporally Dependent Manner. Bone In Press.

[21] Ishaug SL, Yaszemski MJ, Bizios R, Mikos AG. Osteoblast Function on Synthetic Biodegradable Polymers. Journal of Biomedical Materials Research 1994;28:1445-1453.

[22] Cheung HS, Haak MH. Growth of osteoblasts on porous calcium phosphate ceramic: an in vitro model for biocompatibility study. Biomaterials 1989;10:63-67.

[23] Massas R, Pitaru S, Weinreb MM. The effects of titanium and hydroxyapatite on osteoblastic expression and proliferation in rat parietal bone cultures. J Dent Res 1993;72:1005-1008.

[24] Ozawa S, Kasugai S. Evaluation of implant materials (hydroxyapatite, glass-ceramics, titanium) in rat bone marrow stromal cell culture. Biomaterials 1996;17:23-29.

[25] Oonishi H. Orthopaedic applications of hydroxyapatite. Biomaterials 1991;12:171-178.

[26] Vrouwenvelder WC, Groot CG, de Groot K. Histological and biochemical evaluation of osteoblasts cultured on bioactive glass, hydroxylapatite, titanium alloy, and stainless steel. J Biomed Mater Res 1993;27:465-475.

[27] Evans EJ. Toxicity of hydroxyapatite in vitro: the effect of particle size. Biomaterials 1991;12:574-576.

[28] Alliot-Licht B, Gregoire M, Orly I, Menanteau J. Cellular activity of osteoblasts in the presence of hydroxyapatite: an in vitro experiment. Biomaterials 1991;12:752-756.

[29] Denhardt DT, Noda M. Osteopontin expression and function: role in bone remodeling. J Cell Biochem Suppl 1998;30-31:92-102.

[30] Boskey AL, Maresca M, Ullrich W, Doty SB, Butler WT, Prince CW. Osteopontin-hydroxyapatite interactions in vitro: inhibition of hydroxyapatite formation and growth in a gelatin-gel. Bone Miner 1993;22:147-159.

[31] Hunter GK, Hauschka PV, Poole AR, Rosenberg LC, Goldberg HA. Nucleation and inhibition of hydroxyapatite formation by mineralized tissue proteins. Biochem J 1996;317 (Pt 1):59-64.

[32] Park EK, Lee YE, Choi JY, Oh SH, Shin HI, Kim KH, et al. Cellular biocompatibility and stimulatory effects of calcium metaphosphate on osteoblastic differentiation of human bone marrow-derived stromal cells. Biomaterials 2004;25:3403-3411.

[33] Oreffo RO, Driessens FC, Planell JA, Triffitt JT. Growth and differentiation of human bone marrow osteoprogenitors on novel calcium phosphate cements. Biomaterials 1998;19:1845-1854.

[34] Glimcher MJ. Mechanism of calcification: role of collagen fibrils and collagen-phosphoprotein complexes in vitro and in vivo. Anat Rec 1989;224:139-153.

[35] Bushinsky DA. Metabolic alkalosis decreases bone calcium efflux by suppressing osteoclasts and stimulating osteoblasts. Am J Physiol 1996;271:F216-222.

2.8 Figures

Figure 1: X-ray Diffractometry. XRD patterns for (a) Zr-ACP and (b) HAP powders

Figure 2: Ion Concentration. (a) Phosphate and (b) calcium ion concentration in growth medium up to 2 days after Zr-ACP and HAP immersion as determined by ion chromatography. Dotted lines represent concentrations for the control. Bars represent the mean ± spread for n = 2.

Figure 3: pH as a function of time. Change in pH of growth medium with addition of Zr-ACP or HAP. Bars represent the mean ± standard error of 4 samples.

Figure 4: Cell Number. Cell number per well as determined by fluorometric quantification of DNA. Zr-ACP, HAP or no mineral was added (10mg per well) at day 0 and cells were assayed at days 3, 7, 10 and 14. Each bar represents the mean ± standard error for n = 8. A single asterisk (*) represents statistical difference from the control ($p < 0.05$).

Figure 5: Cell Number. Cell number per well as determined by fluorometric quantification of DNA. Zr-ACP, HAP or no mineral was added (10mg per well) at (a) day 4 and assayed at days 5, 7 and 14, (b) or added at day 11 and assayed at days 12 and 14. Each bar represents the mean ± standard error for n = 8. A single asterisk (*) represents statistical difference from the control ($p < 0.05$).

Figure 6: Alkaline Phosphatase activity. ALP activity normalized by cell number. Ten mg Zr-ACP or HAP was added per well at either (a) day 4 and assayed at days 5, 7 and 14, (b) or added at day 11 and assayed at days 12 and 14. Each bar represents the mean ± standard error for n = 8. A single asterisk (*) represents statistical difference from the control ($p < 0.05$).

Figure 7: Osteopontin expression. (a) Bands for osteopontin and G3PDH are presented for cells cultured at 14 days where Zr-ACP, HAP or no mineral was added at days 0(shown), 4, and 11. Each lane represents protein collected from one well, where each condition was repeated in triplicate. (b) Band densities (relative to G3PDH band densities) are plotted versus addition time of minerals. Each bar represents the mean ± standard error for n = 6. A single asterisk (*) represents statistical difference from the control ($p < 0.05$).

Figure 8: Collagen Synthesis. (a) Collagenous protein as a percentage of the total protein synthesized and (b) counts per minute from collagen protein fractions normalized by mean cell number are plotted versus addition time of minerals. Each bar represents the mean ± standard error for n = 4.

Figure 1

(a)

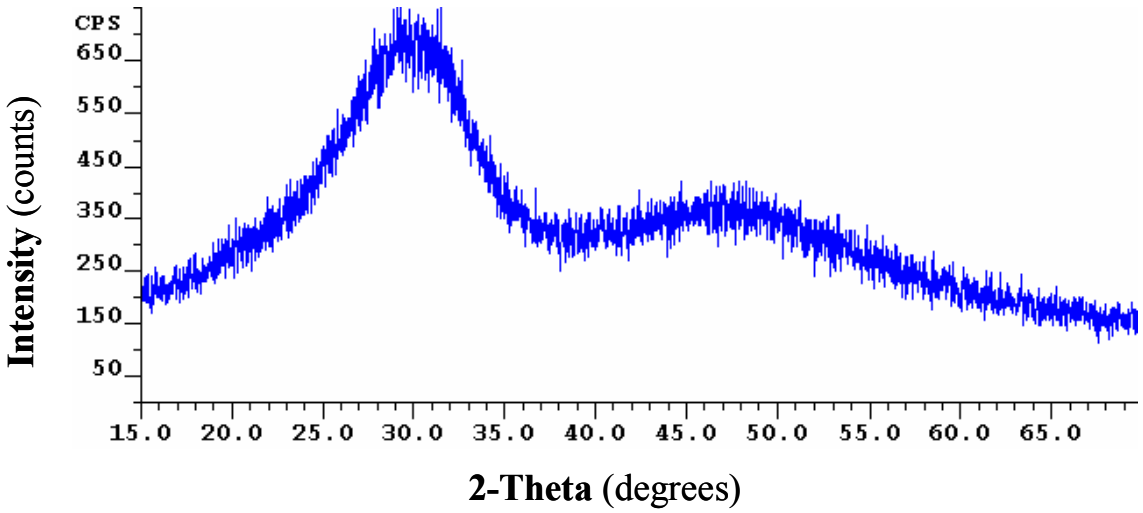
CPS
650
550
450
350
250
150
50
Intensity (counts)
15.0 20.0 25.0 30.0 35.0 40.0 45.0 50.0 55.0 60.0 65.0
2-Theta (degrees)

(b)

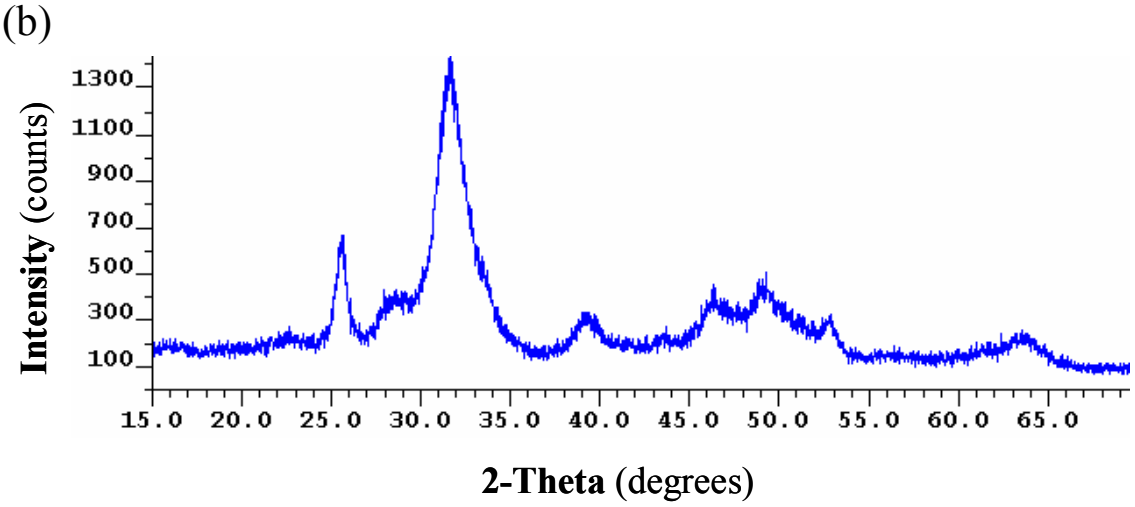
1300
1100
900
700
500
300
100
Intensity (counts)
15.0 20.0 25.0 30.0 35.0 40.0 45.0 50.0 55.0 60.0 65.0
2-Theta (degrees)

Figure 2

a)

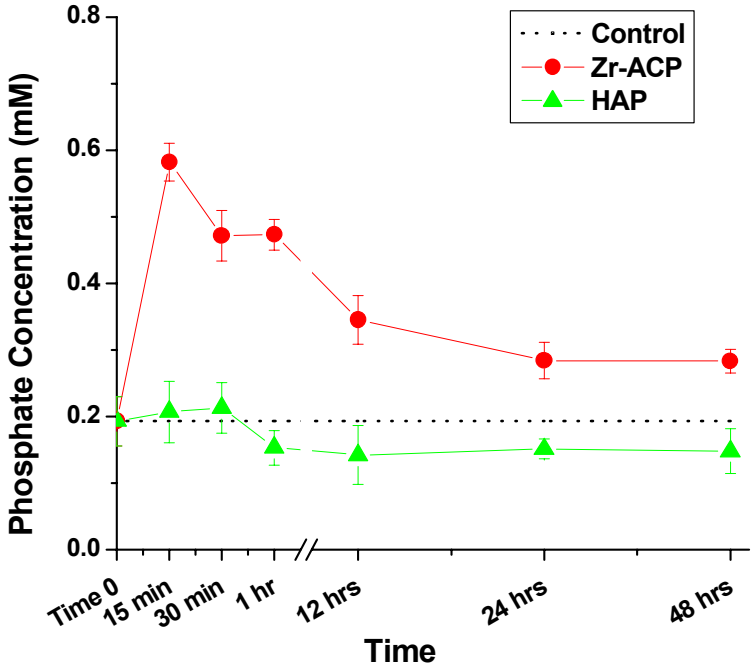
Control
Zr-ACP
HAP
Phosphate Concentration (mM)
0.0
0.2
0.4
0.6
0.8
Time 0
15 min
30 min
1 hr
12 hrs
24 hrs
48 hrs
Time

b)

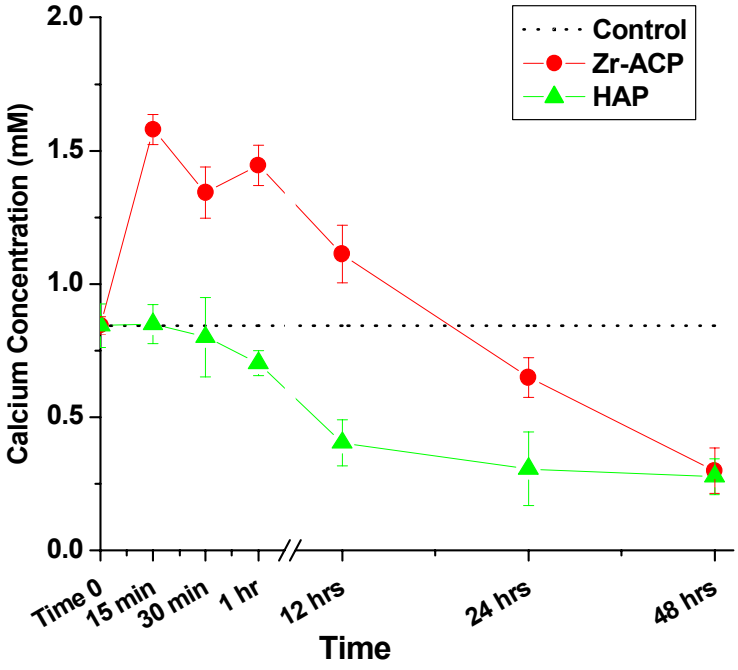
Control
Zr-ACP
HAP
Calcium Concentration (mM)
0.0
0.5
1.0
1.5
2.0
Time 0
15 min
30 min
1 hr
12 hrs
24 hrs
48 hrs
Time

Figure 3

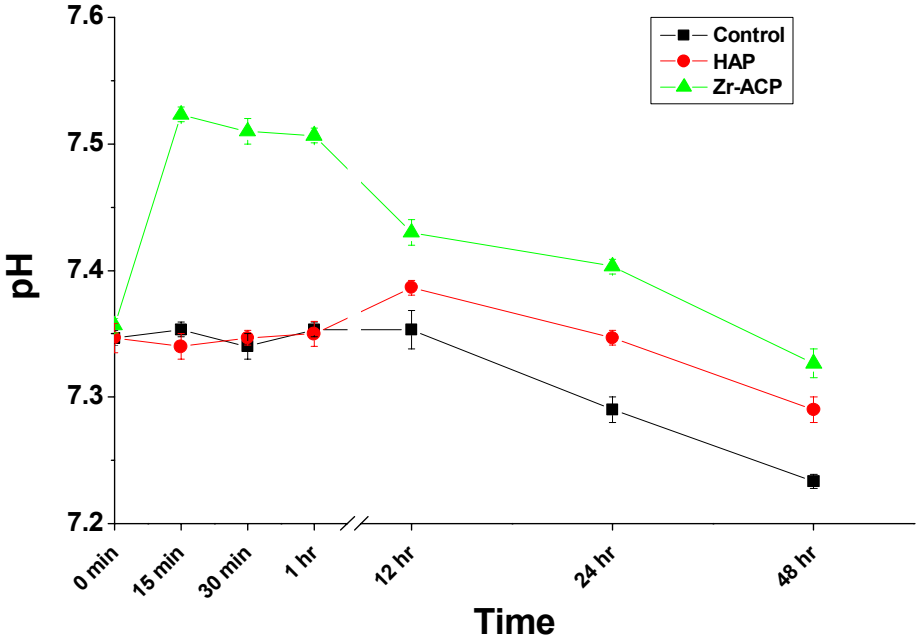
7.6
7.5
7.4
7.3
7.2
pH
Control
HAP
Zr-ACP
0 min
15 min
30 min
1 hr
12 hr
24 hr
48 hr
Time

Figure 4

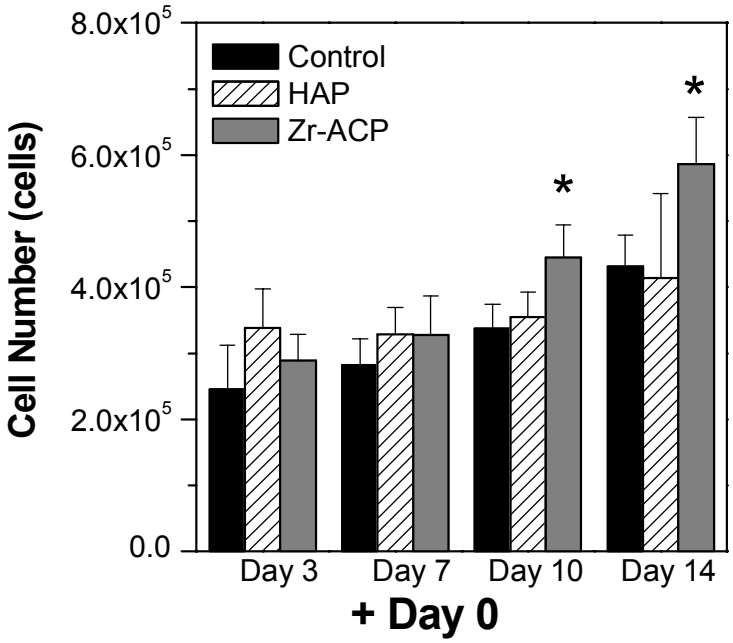
8.0x10^5
6.0x10^5
4.0x10^5
2.0x10^5
0.0
Cell Number (cells)
Control
HAP
Zr-ACP
*
*
Day 3
Day 7
Day 10
Day 14
+ Day 0

Figure 5

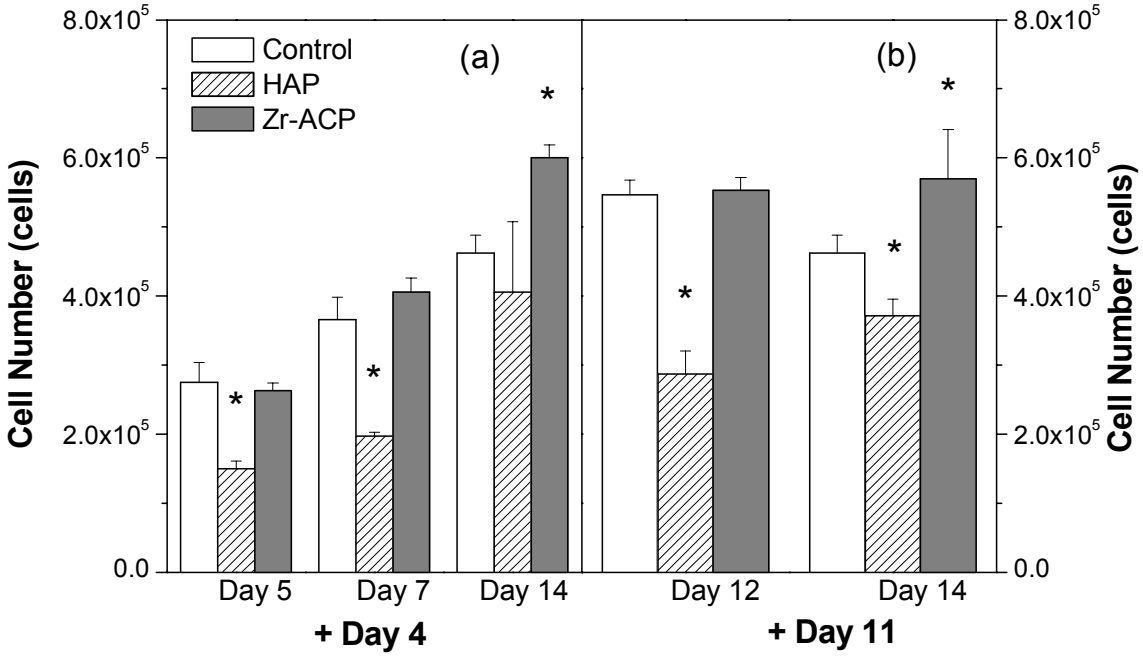
8.0x10^5
6.0x10^5
4.0x10^5
2.0x10^5
0.0
Cell Number (cells)
Control
HAP
Zr-ACP
(a)
(b)
*
Day 5
Day 7
Day 14
Day 12
Day 14
+ Day 4
+ Day 11

Figure 6

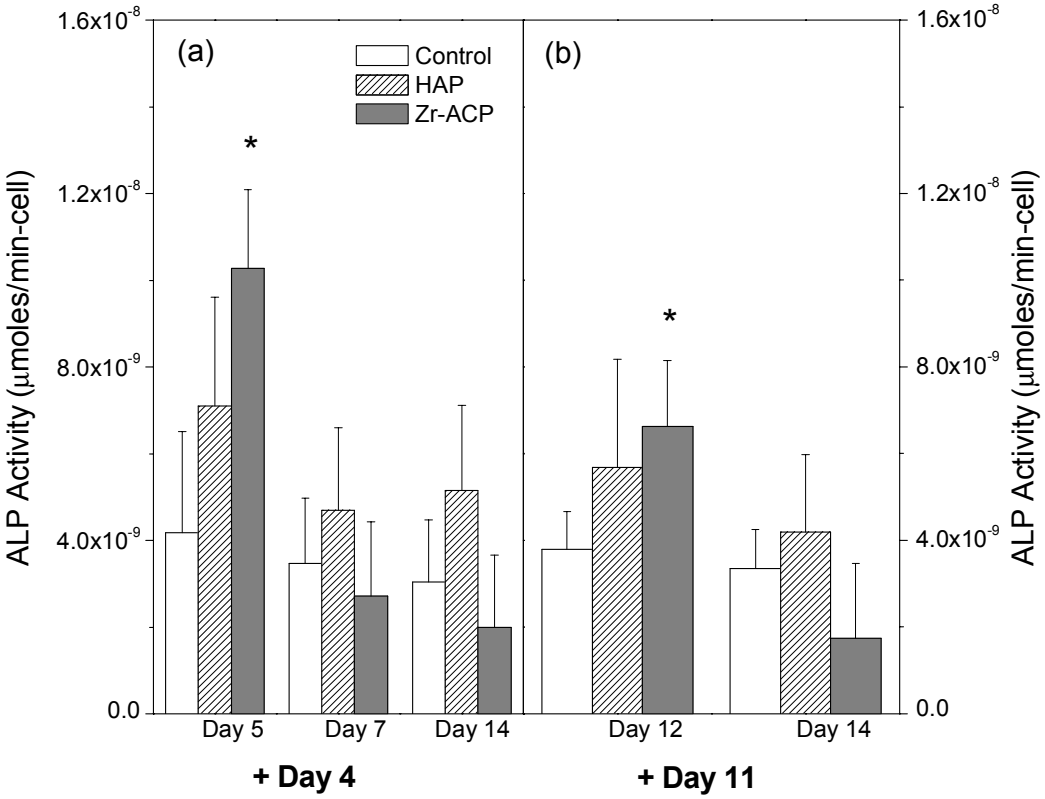
1.6x10-8
1.2x10-8
8.0x10-9
4.0x10-9
0.0
ALP Activity (μmoles/min-cell)
(a)
(b)
Control
HAP
Zr-ACP
*
*
Day 5
Day 7
Day 14
Day 12
Day 14
+ Day 4
+ Day 11

Figure 7

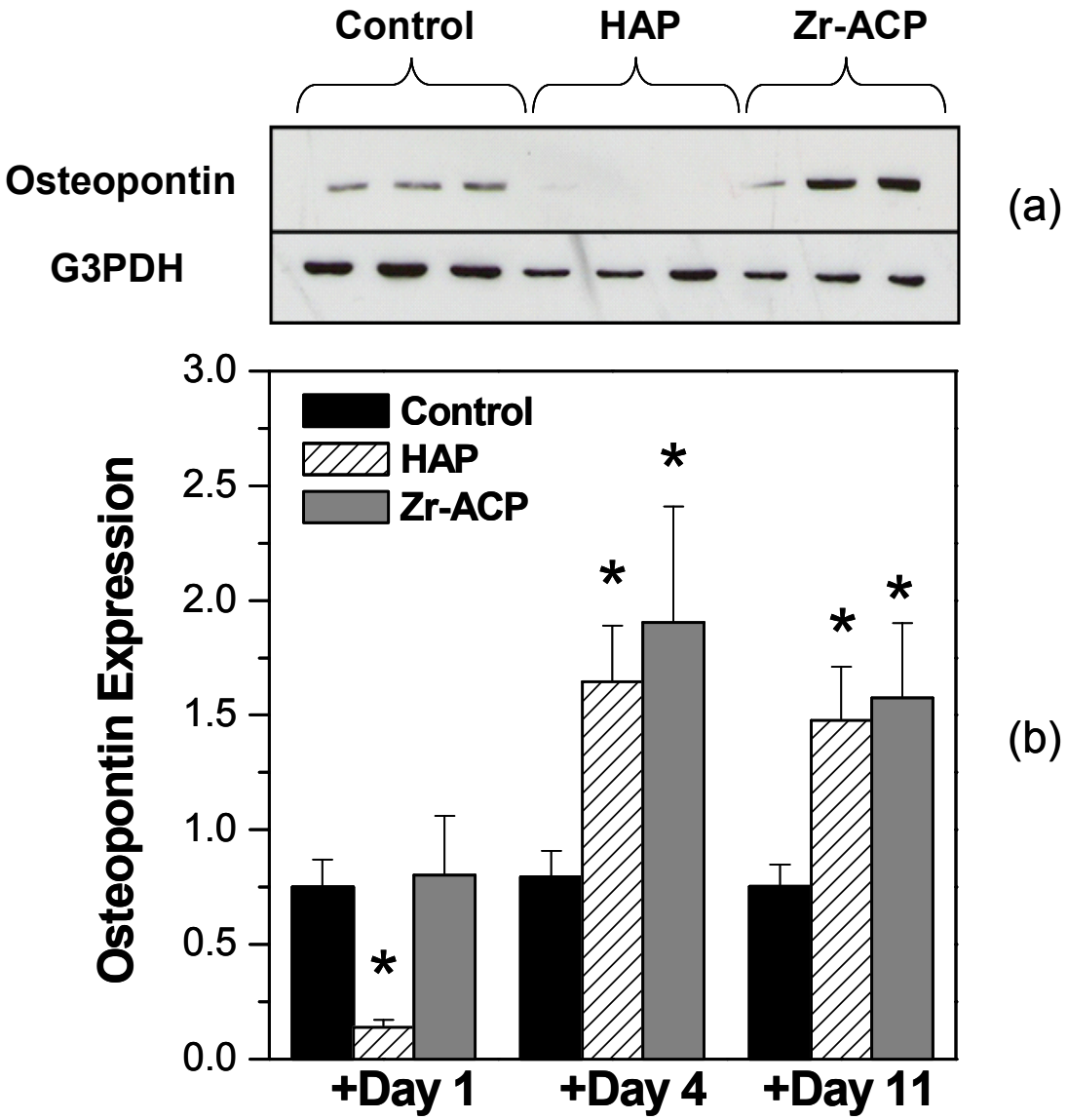
Control
HAP
Zr-ACP
Osteopontin
G3PDH
(a)
Osteopontin Expression
3.0
2.5
2.0
1.5
1.0
0.5
0.0
Control
HAP
Zr-ACP
*
+Day 1
+Day 4
+Day 11
(b)

Figure 8

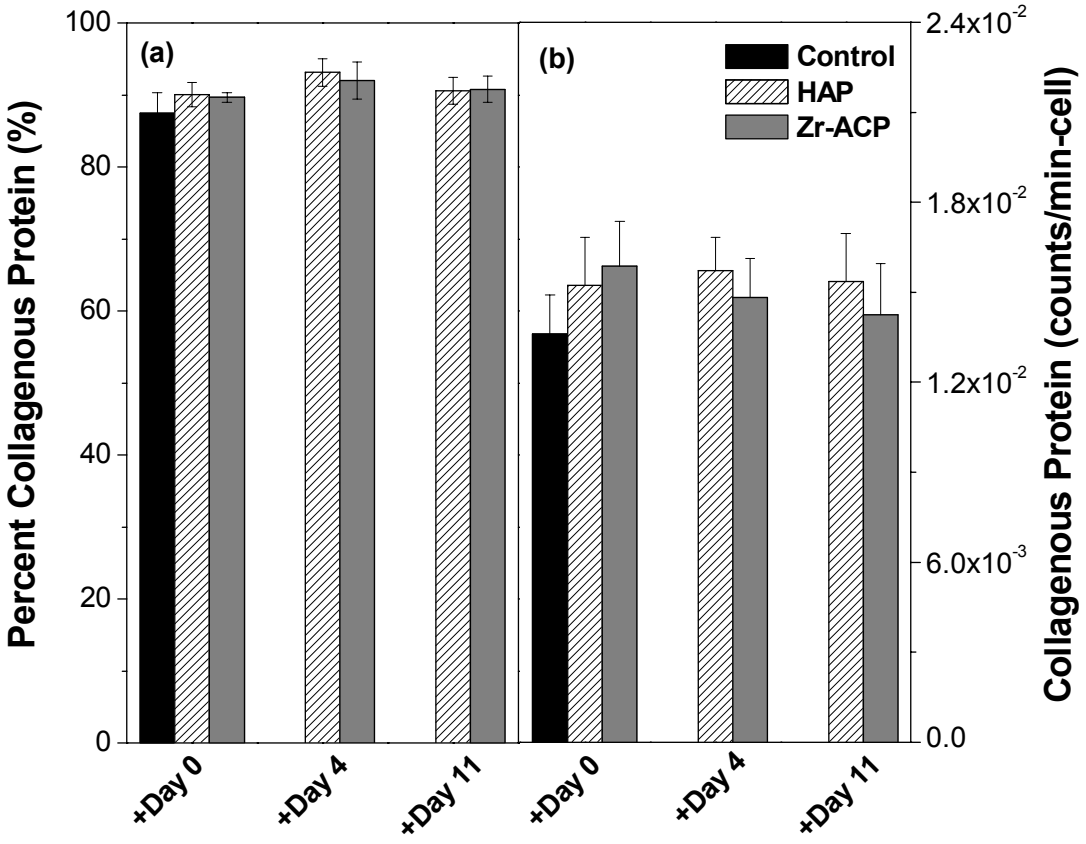
(a)
(b)
Control
HAP
Zr-ACP
Percent Collagenous Protein (%)
Collagenous Protein (counts/min-cell)
100
80
60
40
20
0
2.4x10-2
1.8x10-2
1.2x10-2
6.0x10-3
0.0
+Day 0
+Day 4
+Day 11
+Day 0
+Day 4
+Day 11

Chapter 3: Fabrication and Characterization of Poly(DL lactic-co-glycolic acid)/Zirconia-Hybridized Amorphous Calcium Phosphate Composites

Bryce M. Whited[1], Aaron S. Goldstein[1,2], Drago Skrtic[4], Brian J. Love[1,3]

[1]School of Biomedical Engineering and Sciences, Departments of
[2]Chemical and [3]Materials Science and Engineering
Virginia Polytechnic Institute and State University Blacksburg, VA 24061-0211
[4]American Dental Association Foundation, Paffenbarger Research Center, National Institute of Standards and Technology, 100 Bureau Drive Stop 8546, Gaithersburg, MD 20899

3.1 Abstract

Recently, hydroxyapatite (HAP) and β-tricalcium phosphate (β-TCP) have been incorporated into bioresorbable polyester bone scaffolds to increase the osteoconductivity of bone scaffolds both in vitro and in vivo. Although HAP and β-TCP are osteoconductive, there is no evidence that these materials are osteoinductive. Calcium and phosphate ions, on the other hand, have been postulated to be factors that increase osteoblast differentiation and mineralization. Recently, a zirconia-hybridized pyrophosphate stabilized amorphous calcium phosphate (Zr-ACP) has been synthesized which permits controlled release of calcium and phosphate ions and thus, when incorporated into a bioresorbable scaffold, has great potential to add osteoinductive factors to the scaffold. In this study, highly porous poly(DL lactic-co-glycolic acid) (PLGA) scaffolds were formed by thermal phase separation incorporating Zr-ACP.

Scanning electron microscopy revealed a highly porous structure with pores ranging in size from a few microns to about 100 μm. Zr-ACP particles were evenly

dispersed in the composite structure and were incorporated into the pore walls. The amorphous structure of the Zr-ACP was maintained during composite fabrication as confirmed by X-ray diffraction measurements. Composite scaffolds showed significantly greater compressive yield strengths and moduli as compared to pure polymer scaffolds. These results demonstrate that PLGA/Zr-ACP composites may serve as promising bone scaffolds for bone tissue engineering.

3.2 Introduction

Tissue engineered scaffolds offer a promising alternative to autografts and allografts, both of which have their associated problems and limitations for use as bone replacements [1]. Consequently, many synthetic scaffold materials are currently being investigated to regenerate bone tissue. Among these materials are biodegradable polymers (i.e., polylactic and polyglyclolic acids) and calcium phosphate based materials (i.e., hydroxyapatite and β-tricalcium phosphate) due to their good biocompatibility and osteoconductivity.

Synthetic biodegradable polymers, such as poly(DL lactic-co-glycolic acid) (PLGA), have been used for scaffolds to regenerate bone [2-5]. PLGA has good biocompatibility, the ability to degrade into harmless monomer units, and a useful range of mechanical properties and degradation rates (depending on the copolymer ratio) [2]. PLGA scaffolds have been fabricated with open pore structures that allow cell seeding, attachment, growth and extracellular matrix production in vitro [2] and are replaced by new bone tissue when implanted into bone defects [3]. A porosity ranging from 75% to 90% is preferable for PLGA bone tissue scaffolds [4, 5] and the ideal range of

pore diameters for these scaffolds of 150 - 710 μm has been suggested [4]. Porous polymeric scaffolds have been fabricated by many methods, including: solvent evaporation [6], compression molding [7], gas foaming [8, 9], solution casting/salt leaching [10-12] and phase separation [13-17].

Calcium phosphate ceramics have also been extensively investigated for use as bone scaffolds and bone replacements [18-20]. Most calcium phosphate biomaterials are polycrystalline ceramics characterized by a high biocompatibility, the ability to undergo osseointegration, and varying degrees of resorbablility [20]. Synthetic hydroxyapatite (HAP) and β-tricalcium phosphate (β-TCP) are the two most commonly used calcium phosphate materials for bone replacements due to their good osteoconductivity. Amorphous calcium phosphates, conversely, have been used sparingly as bone replacements, mainly because of rapid and uncontrolled dissolution [21, 22]. Recently, amorphous calcium phosphate has been stabilized by pyrophosphate ions ($P_2O_7^{-4}$) and hybridized with zirconium (Zr-ACP) to retard its dissolution and subsequent conversion to HAP in aqueous environments over long periods of time [23, 24]. In addition, Zr-ACP allows for controlled release of calcium and phosphate ions; factors that have been postulated to increase osteoblast differentiation and mineralization in vitro [25-28]. Incorporation of Zr-ACP into a bioresorbable scaffold could potentially enhance the osteoinductivity and add mechanical stability to the polymer scaffold.

In this study, porous PLGA/Zr-ACP and PLGA/HAP composite foams (5% or 10% (w/v) polymer/solvent with 25 wt% or 50 wt% calcium phosphates) were fabricated using a thermal phase inversion technique as reported previously [29]. The goals were to form a PLGA/Zr-ACP composite with a porous structure and evenly distribute Zr-ACP

into the scaffold while inhibiting Zr-ACP conversion to HAP during processing. Also, a minimum compressive modulus of 50 MPa is desired to mimic human trabecular bone [30]. X-ray diffractometry was employed to determine Zr-ACP crystallinity after composite fabrication. Pore size, pore distribution and mechanical properties of composites were also determined.

3.3 Materials and Methods

3.3.1 Zr-ACP Synthesis

Calcium nitrate tetrahydrate [$Ca(NO_3)_2x4H_2O$], dibasic sodium phosphate [Na_2HPO_4], sodium pyrophosphate [$Na_4P_2O_7x10H_2O$] and sodium hydroxide [NaOH] were purchased from Sigma-Aldrich (St. Louis, MO). Ammonium hydroxide and acetone were purchased from Fisher (Fairlawn, NJ). Zirconyl chloride [$ZrOCl_2$] was purchased from GFS Chemicals (Columbus, OH).

Zr-ACP and HAP were prepared at the American Dental Association Paffenbarger Research Center according to the method of Skrtic et al. [23]. Briefly, for Zr-ACP, a 1.06M solution of a $Ca(NO_3)_2x4H_2O$ was prepared using CO_2-free water (N_2 closed system, designated as solution 1). Forty ml of a 0.25 M $ZrOCl_2$ solution was prepared and designated as solution 2. A 1.16M Na_2HPO_4 solution including 0.024M $Na_4P_2O_7x10H_2O$ was made using CO_2-free water (mechanically stirred at 400 rpm) and 67 ml of a 1M NaOH solution was added under N_2 in a covered beaker where pH of 8.5 to 9 was measured (designated as solution 3). Solutions 1 and 2 were added simultaneously to solution 3 under N_2 and mechanically stirred at 400-500 rpm. Precipitation of the Zr-ACP was instantaneous. The solution was allowed to stabilize for

5 minutes, where after precipitates were filtered and washed twice with cold ammoniated water (2% ammonia) and then washed with cold acetone. Zr-ACP was then frozen in a -50^{o}C freezer for one hour and transferred to a VirTis bench top freeze dry system (SP Industries, Inc., Warminster, PA) for 48 hours at a temperature of -70^{o}C and pressure of 5 mTorr. Further characterization of the materials in terms of crystallinity, surface morphology, Ca/PO_4 molar ratios and dissolution/transformation of Zr-ACP is extensively documented in the literature [23, 24].

3.3.2 Scaffold Preparation

PLGA/HAP and PLGA/Zr-ACP composites were fabricated using a similar thermal phase inversion technique as previously reported [29]. Briefly, 75/25 Poly (DL-lactic-co-glycolic acid) (Absorbable Polymers, Pelham, AL, catalog # 75DG0651) was dissolved in 1, 4 dioxane (Sigma Aldrich, St. Louis, MO) to a 5% or 10% (w/v) solution. Samples were heated at 50^{o}C for 2 hours with stirring to obtain homogeneous polymer solution. Equal volumes of polymer solution were placed into individual wells of a 24-well cell culture plate (Corning, Corning, NY) and Zr-ACP or HAP were added to make a 25% or 50% (w/v) mineral final concentration. Minerals were then evenly dispersed by sonication for 20 s at 8 W (sonic dismembrator 60, Fisher Scientific, Fairlawn, NJ). The samples were transferred to a -50^{o}C ethanol bath for one hour to induce solid-liquid phase separation. The samples were maintained in the freezer at -50^{o}C overnight and then freeze dried using VirTis bench top freeze dry system (SP Industries, Inc., Warminster, PA) for 3 days at a temperature of -70^{o}C and pressure of 5 mTorr.

3.3.3 Morphology Characterization

The morphology of the scaffolds were determined by scanning electron microscopy (SEM). Samples were immersed in liquid nitrogen for several minutes then freeze-fractured with a razor blade in a longitudinal manner (parallel to the direction of solidification). The samples were then sputter coated with 20 nm Pd (Model 208HR; Cressington Scientific Instruments, Cranberry Township, PA) equipped with a thickness controller (Model MTM20; Cressington). Samples were then visualized using a LEO 1550 Field Emission SEM (Carl Zeiss SMT**,** Thornwood, NY) and micrographs obtained using the LEO image software.

3.3.4 Pore Size

The pore size and pore size distribution of the scaffolds were analyzed using public domain Scion Image program (*http://www.scioncorp.com*) and by following the method as previously described [31]. Briefly, a 0.25 mm^2 area of the SEM was selected for image analysis (Figure 1a). Next, contrast and brightness were adjusted to the same level for each SEM image because pore size analysis is determined by grayscale of the image (Figure 1b). Thresholding was performed at a set value for each image (Figure 1c) and then compared to the original image (Figure 1a) with respect to pore size and position to validate the thresholding level. If the threshold image did not match the original image, thresholding was repeated until a good match was obtained between the original and threshold image. After calibrating with a known scale, each pore was labeled and measured (Figure 1d) where after the data was exported to an Excel

spreadsheet for further analysis. Pore diameter was determined by averaging the major and minor axes. Area was determined by using the following formula:

$$A = \frac{(\pi \times \text{major axis} \times \text{minor axis})}{4}$$

3.3.5 X-ray Diffractometry

The crystallinity of the lyophilized solids and composites were verified by X-ray diffractometry (XRD). The XRD profiles were recorded in the range of 15^o to 70^o with CuKα X-ray source (λ=1.54Å) using a XDS 2000 (Scintac Inc., USA) operated at 40kV and 40mA. The samples were step scanned in intervals of 0.020^o at a scanning speed of 2.000^o/min.

3.3.6 Mechanical Properties

The compressive modulus and yield strength of the composites were determined using a Instron 4204 with a 1kN static load cell (Instron, Canton, MA) as described previously [29]. The top layer of the foam disks were trimmed off with a razor blade to achieve a desired thickness of 3 mm. The final dimensions of the composites were 16 mm in diameter and 3 mm in thickness. The compression tests were carried out at using a crosshead speed of 0.5 mm/min. Modulus was determined by the initial slope of the stress-strain curve. Yield strength was determined by using a parallel 0.02% strain offset. Three samples were tested for each condition.

3.3.7 Statistical Analysis

Values are presented as mean ± standard deviation. Statistical analysis was performed using Origin® 6.1 (OriginLab, Northampton, MA). A one-way analysis of variance (ANOVA) procedure with a significance level (α) of 0.05 was used to determine significant differences between groups.

3.4 Results and Discussion

3.4.1 Composite Morphology

Porous PLGA/HAP and PLGA/Zr-ACP composites were fabricated using a thermally induced solid-liquid phase separation and subsequent sublimation of the solvent. Size of HAP particles used ranged from about 0.5 to 10 microns (Figure 2a), whereas average Zr-ACP particle size was less than one micron (Figure 2b). Pore size ranged from 3.3 μm to 114.7 μm for the 10% PLGA scaffold (Figures 4a, 4b) and from 1.8 μm to 32.5 μm for 5% PLGA scaffolds (Figure 4c, 4d) with average pore sizes of 20.9 μm and 4.3 μm respectively (Table 1). Although the average pore size seems very small for these scaffolds, the pore area distribution shows that 87% of the pore area is comprised from pores with average diameters greater than 50 μm for the 10% PLGA scaffold (Figure 3).

PLGA/Zr-ACP 75:25 composites were fabricated from 5% and 10% polymer solutions with pore sizes ranging from 2.9 μm to 107.2 μm and 3.6 μm to 154.4 μm respectively (Figures 5a – 5d). As scaffolds increased in Zr-ACP content (50:50 blends as compared to 75:25 blends), average pore size decreased from 46.8 μm to 6.28 μm respectively and pore morphology was more irregular (Figures 6a - 6d). All scaffolds

including HAP displayed irregular pore architecture with average pore sizes ranging from 2.5 μm to 9.5 μm (Figures 7 and 8). One explanation for smaller and more irregular pores for the PLGA/HAP scaffolds could be that the HAP particles used are larger than the Zr-ACP particles. These findings are consistent with results of a previous study where nano-hydroxyapatite particles, average size less than one micron, and hydroxyapatite particles, average size of 10 μm, were incorporated into a PLLA scaffold using a similar phase inversion technique [32]. Results from this study show that the scaffold with nano-hydroxyapatite particles have much larger pores and a more regular pore morphology than scaffolds fabricated with larger hydroxyapatite particles [32].

Adhesion between the Zr-ACP particles and PLGA matrix are observed (Figure 9) and the surface of the pore walls show even dispersion and inclusion of the Zr-ACP particles, which range in size from less than one to 5 microns for a representative PLGA/Zr-ACP scaffold (Figure 9). Incorporation of Zr-ACP in the pore walls could increase osteoconductivity of the composite for use as a bone scaffold.

Although these structures show to be highly porous, no indication of pore interconnectivity was seen for these scaffolds using SEM.

3.4.2 X-ray Diffractometry

XRD patterns for Zr-ACP lack discrete diffraction peaks, indicating an amorphous structure (Chapter 2: Figure 1a). In contrast, HAP shows discrete diffraction peaks indicative of a crystalline structure (Chapter 2: Figure 1b). The amorphous structure of Zr-ACP has been shown to increase dissolution rates and subsequently release more Ca^{+2} and PO_4^{-3} ions in aqueous environments as compared to HAP [23].

These ions have been postulated to regulate osteoblastic differentiation [25, 26] and mineralization [27, 28] in vitro, but the mechanisms by which these factors promote osteogenesis remains unknown. It is therefore important to ensure that Zr-ACP retains its amorphous structure and does not convert to HAP during PLGA/Zr-ACP composite fabrication. The 50:50 PLGA/Zr-ACP composite diffraction pattern lacks discrete diffraction peaks, which is characteristic of amorphous materials (Figure 10a). In contrast, XRD patterns for the 50:50 PLGA/HAP composite shows a semi-crystalline structure as evidenced by discrete diffraction peaks (Figure 10b). This confirms that the Zr-ACP retains its amorphous structure even during the solid-liquid phase separation technique employed in this study.

3.4.3 Mechanical Properties

Compressive yield strength and modulus were determined for 10% PLGA and PLGA/Zr-ACP composite scaffolds. The compressive modulus for the 50:50, 75:25 PLGA/Zr-ACP composites and PLGA foams were 51.9 ± 5.6 MPa, 35.6 ± 8.9 MPa and 14.7 ± 6.8 MPa respectively (Figure 11a). The 50:50 PLGA/Zr-ACP foams met the 50 MPa compressive modulus criterion for replacement of human trabecular bone [30]. Also, a significant increase in compressive yield was obtained by adding Zr-ACP to the structure: 0.138 ± 0.013 MPa (50:50) and 0.078 ± 0.0097 MPa (75:25) as compared to 0.035 ± 0.0065 MPa (Figure 11b). Previous studies have shown that 5% polymer 50:50 poly(lactic acid)/HAP composites have a compressive yield strength and modulus of about 0.040 MPa and 12 MPa respectively [29]. The increase in mechanical stability of our structures was probably due to the increase in polymer concentration (10% as

compared to 5%). These results show that incorporation of Zr-ACP has a significant effect on the mechanical properties of the composite as compared to PLGA alone.

3.5 Conclusions

In this study, a thermal solid-liquid phase separation technique was used to fabricate PLGA/Zr-ACP scaffolds. Structures displayed a porous morphology with pore sizes ranging from 3.6 μm to 154.4 μm for composites with 25% (w/v) Zr-ACP using a 10% (w/v) PLGA/dioxane mixture. SEM images showed adhesion between PLGA matrix and Zr-ACP in addition to even dispersion and inclusion of Zr-ACP in the pore walls of the structure. XRD analysis confirmed that Zr-ACP retained its amorphous structure during composite fabrication. 50:50 PLGA/Zr-ACP composites achieved a compressive modulus of 51.9 ± 5.6 MPa whereas PLGA structures had a modulus of only 14.7 ± 6.8 MPa. These studies demonstrate that Zr-ACP can be incorporated into a porous biodegradable polymer composite that could be useful for bone scaffolds that require load bearing.

3.6 References

[1] Khan SN, Cammisa FP, Sandhu HS, Diwan AD, Girardi FP, Lane JM. The biology of bone grafting. J Am Acad Orthop Surg 2005;13:77-86.

[2] Ishaug SL, Yaszemski MJ, Bizios R, Mikos AG. Osteoblast function on synthetic biodegradable polymers. Journal of Biomedical Materials Research 1994;28:1445-1453.

[3] Ishaug SL, Crane GM, Miller MJ, Yasko AW, Yaszemski MJ, Mikos AG. Bone formation by three-dimensional stromal osteoblast culture in biodegradable polymer scaffolds. Journal of Biomedical Materials Research 1997;36:17-28.

[4] Ishaug-Riley SL, Crane-Kruger GM, Yaszemski MJ, Mikos AG. Three-dimensional culture of rat calvarial osteoblasts in porous biodegradable polymers. Biomaterials 1998;19:1405-1412.

[5] Lo H, Kadiyala S, Guggino SE, Leong KW. Poly(l-lactic acid) foams with cell seeding and controlled-release capacity. J Biomed Mater Res 1996;30:475-484.

[6] Hu Y, Grainger DW, Winn SR, Hollinger JO. Fabrication of poly(alpha-hydroxy acid) foam scaffolds using multiple solvent systems. J Biomed Mater Res 2002;59:563-572.

[7] Mikos AG, Bao Y, Cima LG, Ingber DE, Vacanti JP, Langer R. Preparation of poly(glycolic acid) bonded fiber structures for cell attachment and transplantation. Journal of Biomedical Materials Research 1993;27:183-189.

[8] Mooney DJ, Baldwin DF, Suh NP, Vacanti LP, Langer R. Novel approach to fabricate porous sponges of poly(d,l-lactic-co-glycolic acid) without the use of organic solvents. Biomaterials 1996;17:1417-1422.

[9] Nam YS, Yoon JJ, Park TG. A novel fabrication method of macroporous biodegradable polymer scaffolds using gas foaming salt as a porogen additive. J Biomed Mater Res 2000;53:1-7.

[10] Hu YH, Grainger DW, Winn SR, Hollinger JO. Fabrication of poly(a-hydroxy acid) foam scaffolds using multiple solvent systems, 2002.p. 563-572.

[11] Tsuji H, Smith R, Bonfield W, Ikada Y. Porous biodegradable polyesters. I. Preparation of porous poly(l-lactide) films by extraction of poly(ethylene oxide) from their blends. In: Journal of Applied Polymer Science; 2000. p. 629-637.

[12] Wake MC, Gupta PK, Mikos AG. Fabrication of pliable biodegradable polymer foams to engineer soft tissues. In: Cell Transplantation; 1996. p. 465-473.

[13] Zoppi RA, Contant S, Duek EAR, Marques FR, Wada MLF, Nunes SP. Porous poly(l-lactide) films obtained by immersion precipitation process: Morphology, phase separation and culture of vero cells. In: Polymer; 1999. p. 3275-3289.

[14] Lo H, Kadiyala S, Guggino SE, Leong KW. Poly(l-lactic acid) foams with cell seeding and controlled-release capacity. In: Journal of Biomedical Materials Research; 1996. p. 475-484.

[15] Schugens C, Maquet V, Grandfils C, Jerome R, Teyssie P. Biodegradable and macroporous polylactide implants for cell transplantation .1. Preparation of macroporous polylactide supports by solid-liquid phase separation. In: Polymer; 1996. p. 1027-1038.

[16] Schugens C, Maquet V, Grandfils C, Jerome R, Teyssie P. Polylactide macroporous biodegradable implants for cell transplantation .2. Preparation of polylactide foams by liquid-liquid phase separation. In: Journal of Biomedical Materials Research; 1996. p. 449-461.

[17] Gutsche AT, Lo HN, Zurlo J, Yager J, Leong KW. Engineering of a sugar-derivatized porous network for hepatocyte culture. In: Biomaterials; 1996. p. 387-393.

[18] Schmitz JP, Hollinger JO, Milam SB. Reconstruction of bone using calcium phosphate bone cements: A critical review. J Oral Maxillofac Surg 1999;57:1122-1126.

[19] Saffar JL, Colombier ML, Detienville R. Bone formation in tricalcium phosphate-filled periodontal intrabony lesions. Histological observations in humans. J Periodontol 1990;61:209-216.

[20] Goshima J, Goldberg VM, Caplan AI. Osteogenic potential of culture-expanded rat marrow cells as assayed in vivo with porous calcium phosphate ceramic. Biomaterials 1991;12:253-258.

[21] Brugge PJ, Wolke JG, Jansen JA. Effect of calcium phosphate coating composition and crystallinity on the response of osteogenic cells in vitro. Clin Oral Implants Res 2003;14:472-480.

[22] Maxian SH, Zawadsky JP, Dunn MG. In vitro evaluation of amorphous calcium phosphate and poorly crystallized hydroxyapatite coatings on titanium implants. J Biomed Mater Res 1993;27:111-117.

[23] Skrtic D, Antonucci JM, Eanes ED, Brunworth RT. Silica- and zirconia-hybridized amorphous calcium phosphate: Effect on transformation to hydroxyapatite. J Biomed Mater Res 2002;59:597-604.

[24] Skrtic D, Antonucci JM, Eanes ED, Eidelman N. Dental composites based on hybrid and surface-modified amorphous calcium phosphates. Biomaterials 2004;25:1141-1150.

[25] Lossdorfer S, Schwartz Z, Lohmann CH, Greenspan DC, Ranly DM, Boyan BD. Osteoblast response to bioactive glasses in vitro correlates with inorganic phosphate content. Biomaterials 2004;25:2547-2555.

[26] Tenenbaum HC, Heersche JN. Differentiation of osteoblasts and formation of mineralized bone in vitro. Calcif Tissue Int 1982;34:76-79.

[27] Chang YL, Stanford CM, Keller JC. Calcium and phosphate supplementation promotes bone cell mineralization: Implications for hydroxyapatite (ha)-enhanced bone formation. J Biomed Mater Res 2000;52:270-278.

[28] Maeno S, Niki Y, Matsumoto H, Morioka H, Yatabe T, Funayama A, et al. The effect of calcium ion concentration on osteoblast viability, proliferation and differentiation in monolayer and 3d culture. Biomaterials 2005;26:4847-4855.

[29] Zhang RY, Ma PX. Poly(alpha-hydroxyl acids) hydroxyapatite porous composites for bone-tissue engineering. I. Preparation and morphology. Journal of Biomedical Materials Research 1999;44:446-455.

[30] Goldstein SA, Matthews LS, Kuhn JL, Hollister SJ. Trabecular bone remodeling: An experimental model. Journal of Biomechanics 1991;24:135-150.

[31] Zhang JY, Doll BA, Beckman EJ, Hollinger JO. A biodegradable polyurethane-ascorbic acid scaffold for bone tissue engineering. Journal of Biomedical Materials Research Part A 2003;67A:389-400.

[32] Wei G, Ma PX. Structure and properties of nano-hydroxyapatite/polymer composite scaffolds for bone tissue engineering. Biomaterials 2004;25:4749-4757.

3.7 Figures and Tables

Figure 1: Thresholding process for a representative PLGA foam composite scaffold. (a) Original SEM image; (b) SEM image after brightness and contrast adjusted; (c) threshold SEM image; and (d) labeled pores of a PLGA foam composite scaffold.

Figure 2: SEM micrographs of (a) HAP and (b) Zr-ACP powders. Original magnification 5000x.

Figure 3: Average pore diameter versus total pore area for PLGA, 75:25 PLGA/Zr-ACP, and 50:50 PLGA Zr-ACP composites made from 10% (w/v) PLGA/dioxane mixture.

Figure 4: SEM micrographs of PLGA foam prepared from (a,b) 10% (w/v) and (c,d) 5% (w/v) PLGA/dioxane mixture. Original magnifications: (a,c) 500x, (b,d) 1000x.

Figure 5: SEM micrographs of 75:25 PLGA/Zr-ACP composites prepared from (a,b) 10% (w/v) and (c,d) 5% (w/v) PLGA/dioxane mixtures. Original magnifications: (a,c) 500x, (b,d) 1000x.

Figure 6: SEM micrographs of 50:50 PLGA/Zr-ACP composites prepared from (a,b) 10% (w/v) and (c,d) 5% (w/v) PLGA/dioxane mixtures. Original magnifications: (a,c) 500x, (b,d) 1000x.

Figure 7: SEM micrographs of 75:25 PLGA/HAP composites prepared from (a,b) 10% (w/v) and (c,d) 5% (w/v) PLGA/dioxane mixtures. Original magnifications: (a,c) 500x, (b,d) 1000x.

Figure 8: SEM micrographs of 50:50 PLGA/HAP composites prepared from (a,b) 10% (w/v) and (c,d) 5% (w/v) PLGA/dioxane mixtures. Original magnifications: (a,c) 500x, (b,d) 1000x.

Figure 9: SEM micrograph of 50:50 PLGA/Zr-ACP composite prepared from 10% (w/v) PLGA/dioxane mixture. Zr-ACp particles are shown incorporated in the pore wall. Original magnification: 5000x.

Figure 10: X-ray diffractometry patterns for a (a) PLGA/Zr-ACP - 50:50 composite and (b) PLGA/HAP - 50:50 composite prepared from 10%(w/v) PLGA/dioxane mixture.

Figure 11: (a) Compressive modulus and (b) yield strength of the PLGA/Zr-ACP composites (labeled: 75:25 and 50:50) and PLGA foams (labeled: PLGA). Each bar represents the mean ± standard error for $n = 3$. A single asterisk (*) represents statistical difference from the PLGA foam ($p < 0.05$).

Table 1: Maximum, minimum and average pore diameter for each fabricated scaffold.

Figure 1

(a)

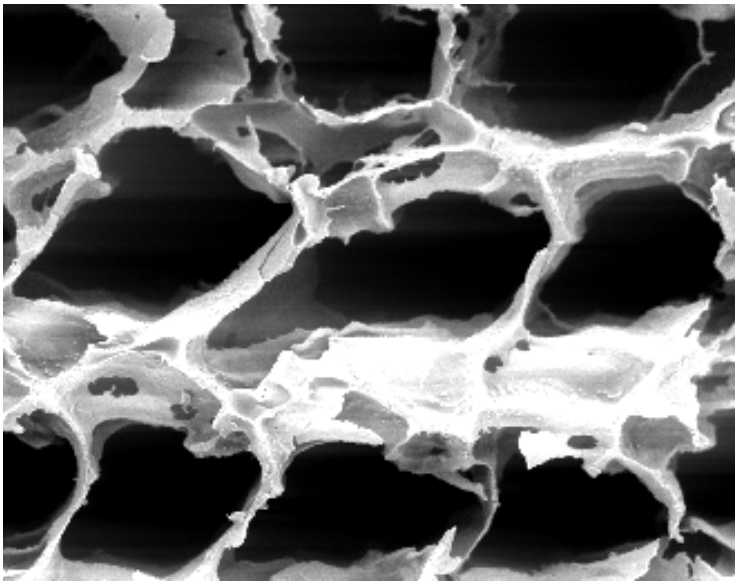

(b)

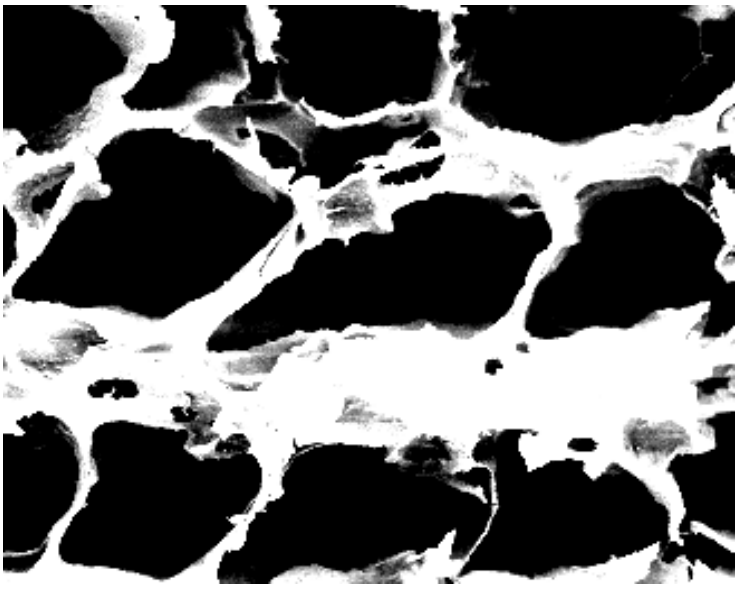

Figure 1

(c)

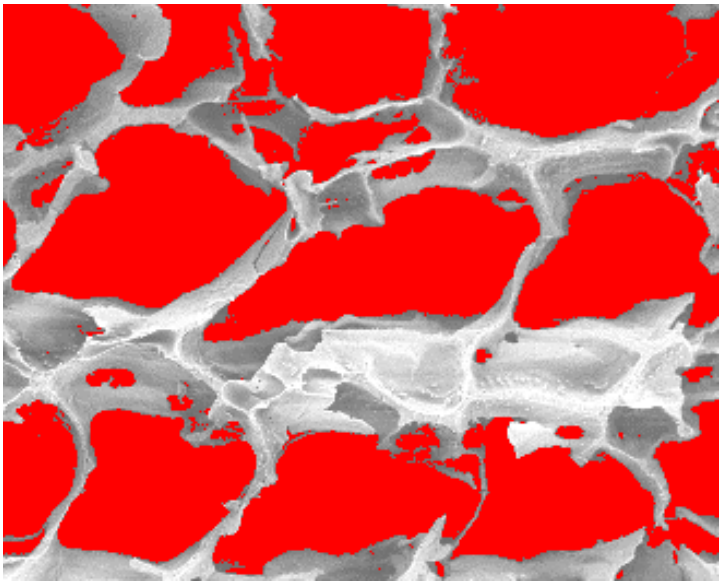

(d)

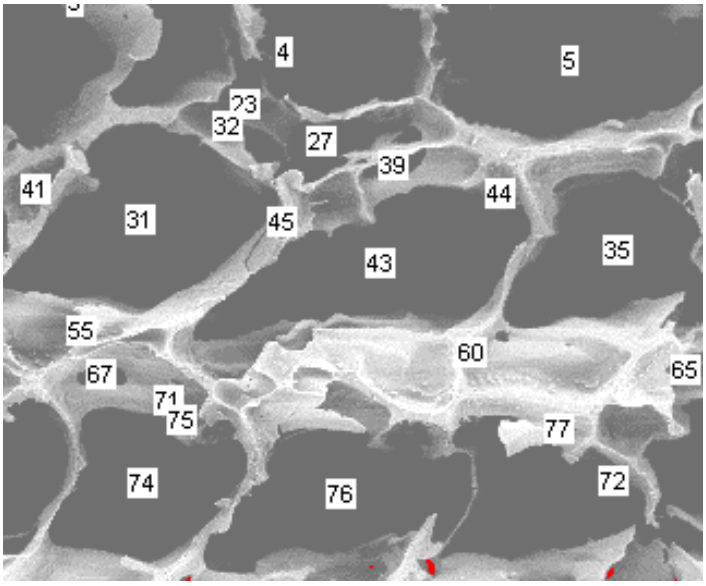

Figure 2

(a)

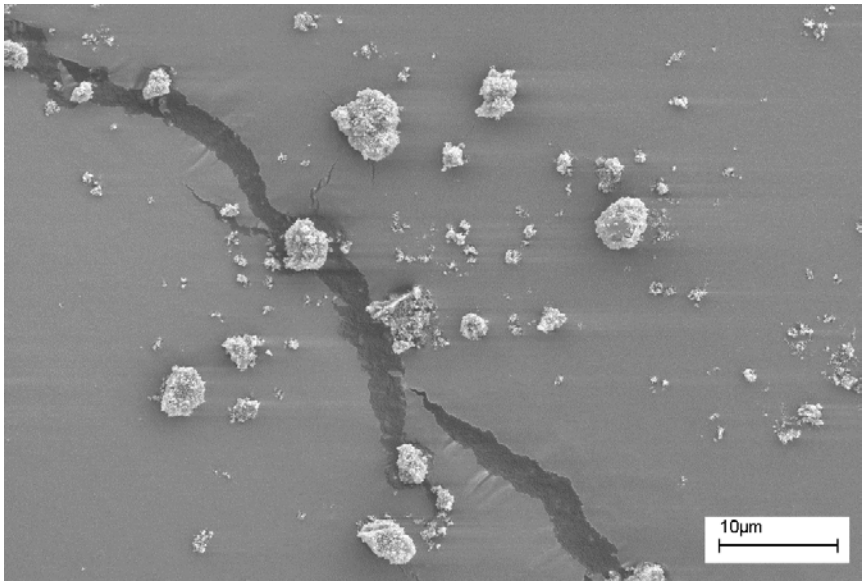

(b)

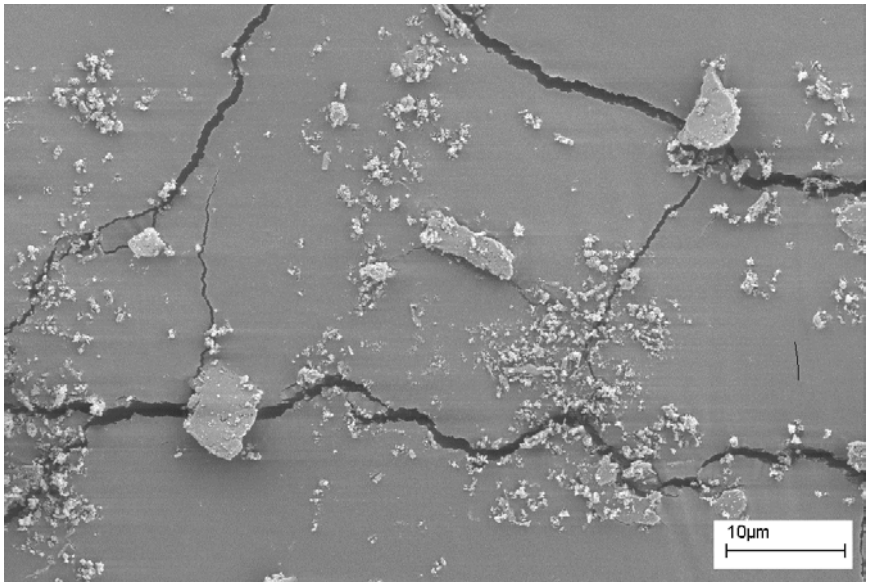

Figure 3

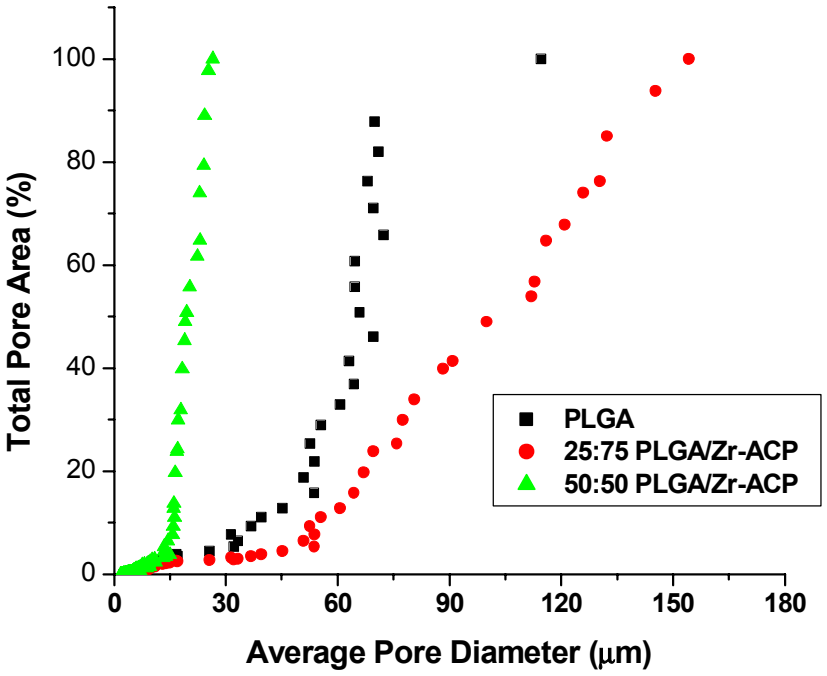
Total Pore Area (%)
Average Pore Diameter (μm)
0
20
40
60
80
100
0
30
60
90
120
150
180
PLGA
25:75 PLGA/Zr-ACP
50:50 PLGA/Zr-ACP

Figure 4

(a)

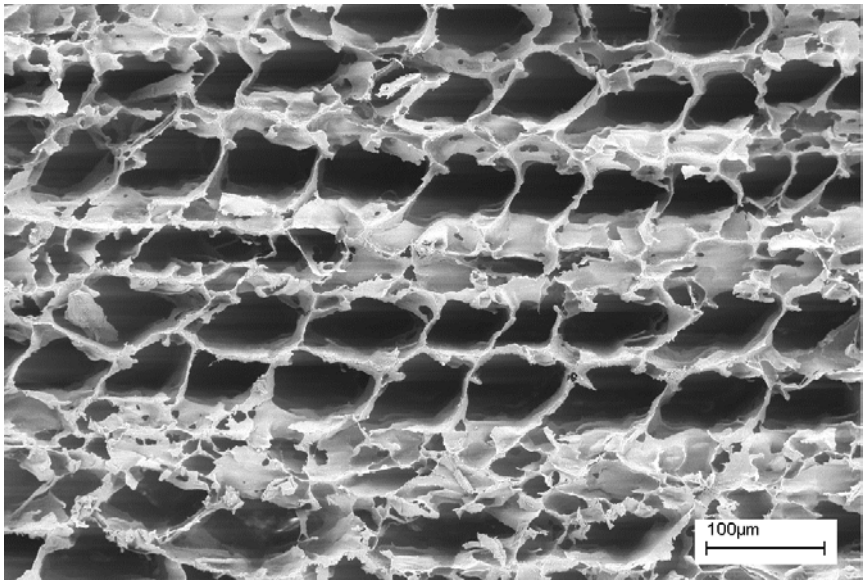

(b)

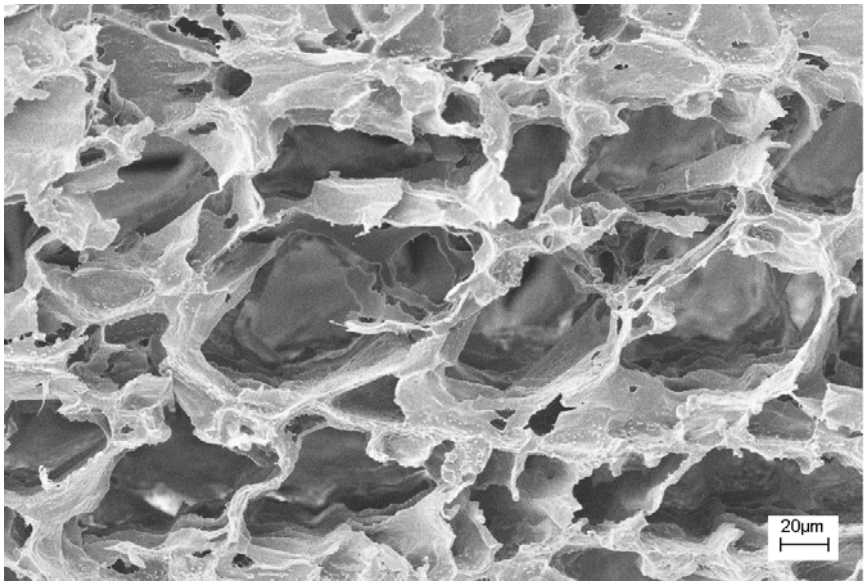

Figure 4

(c)

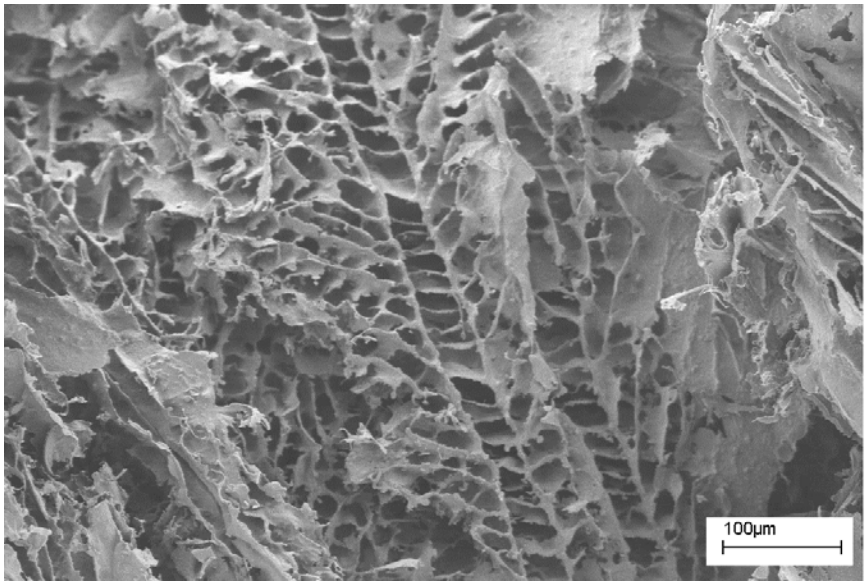

(d)

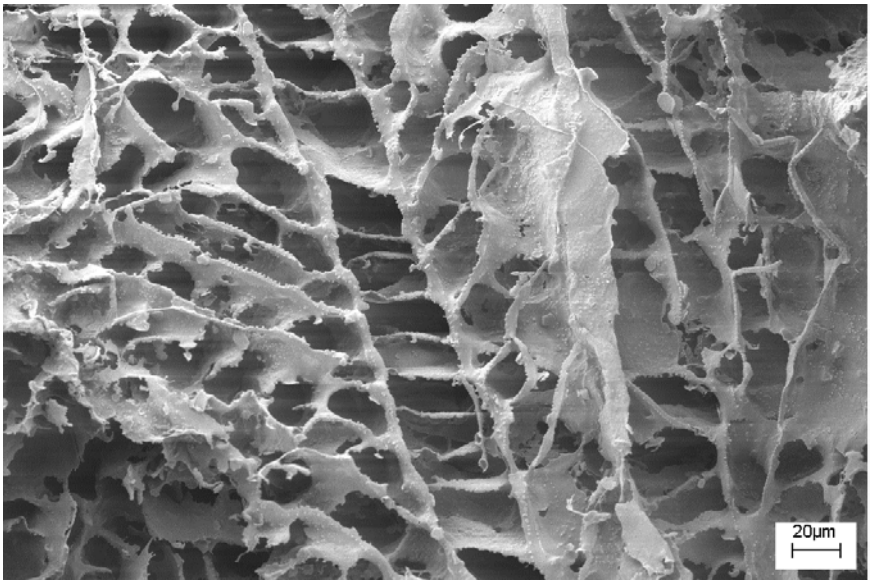

Figure 5

(a)

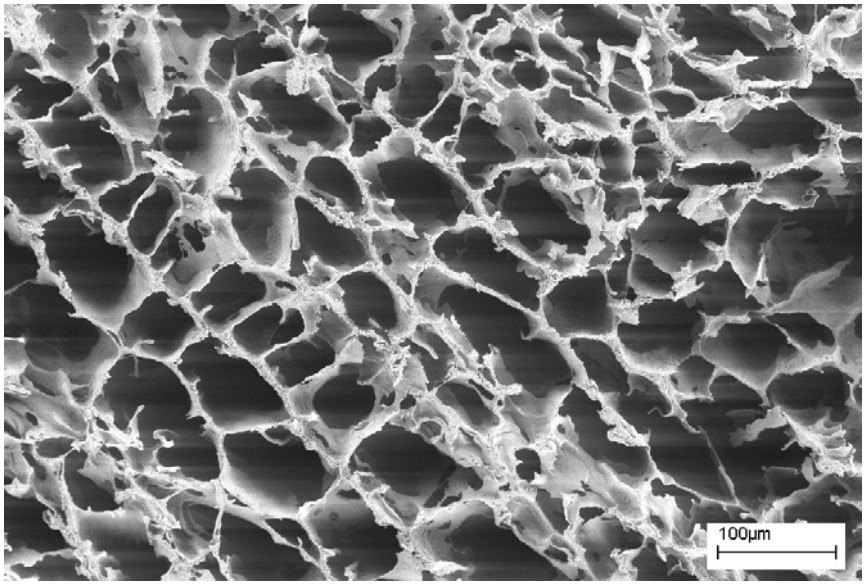

(b)

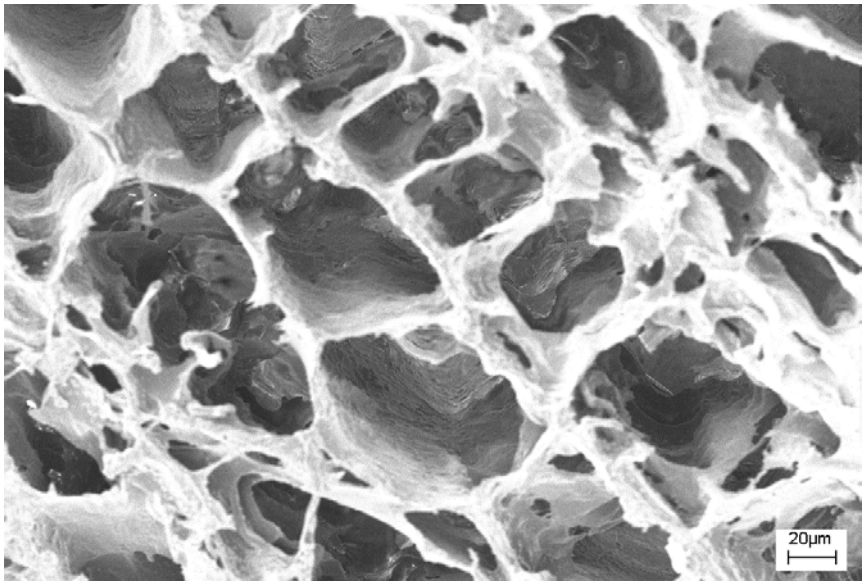

Figure 5

(c)

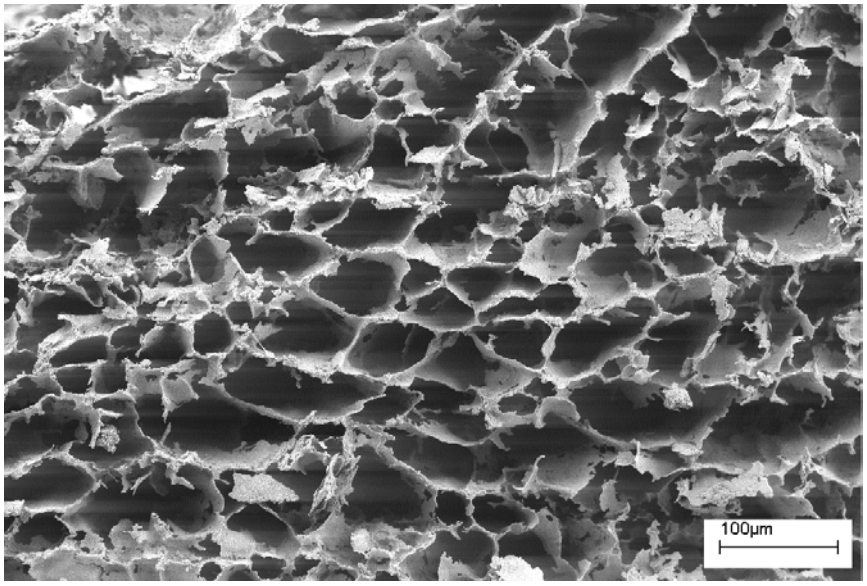

(d)

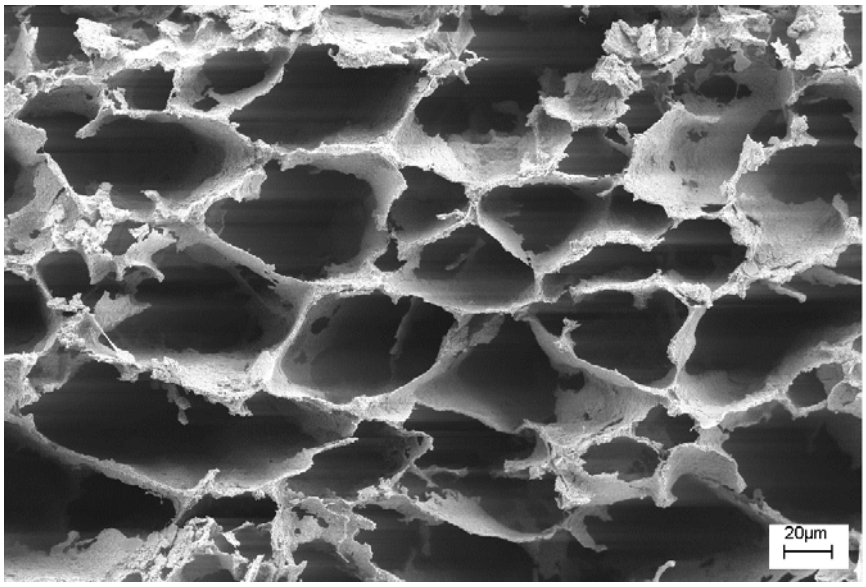

Figure 6

(a)

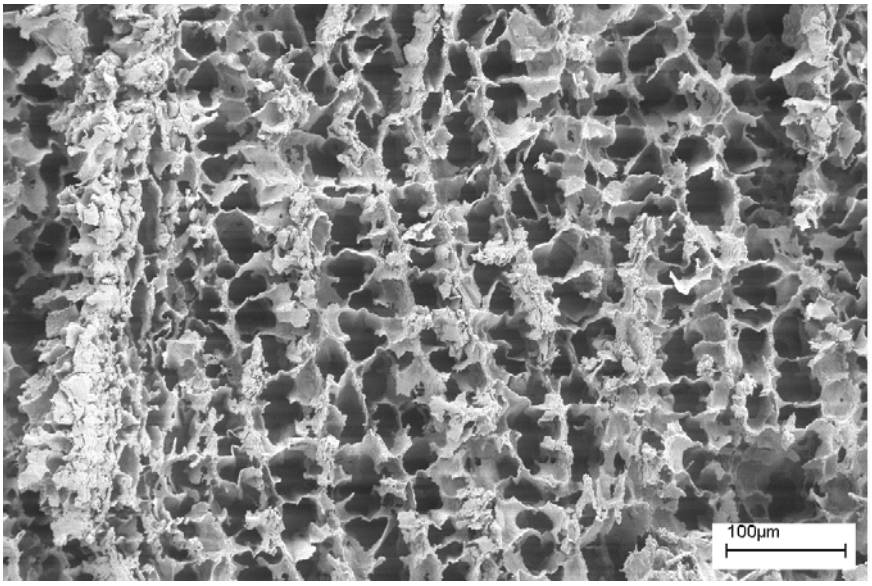

(b)

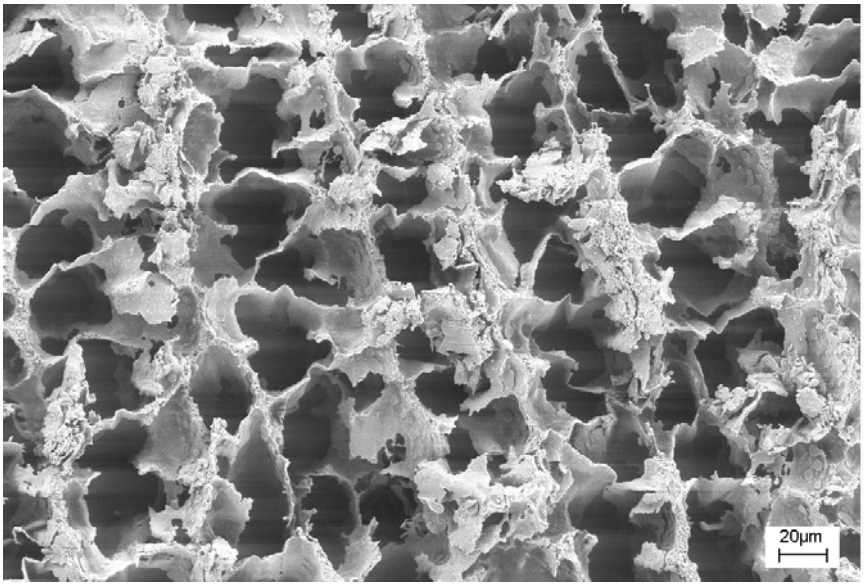

Figure 6

(c)

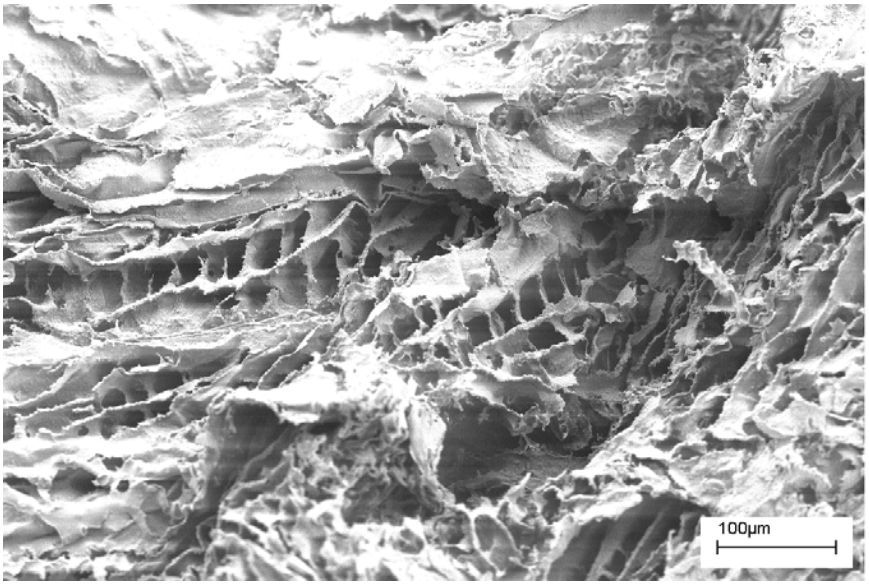

(d)

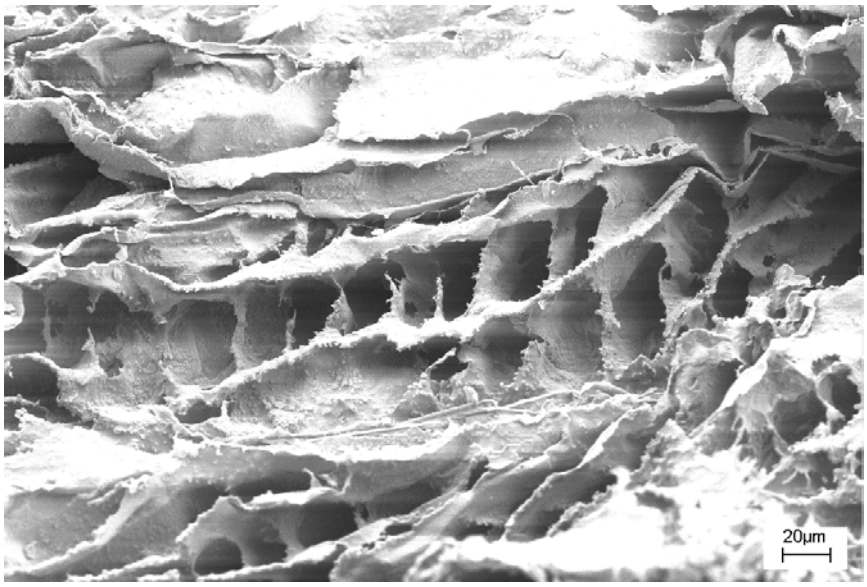

Figure 7

(a)

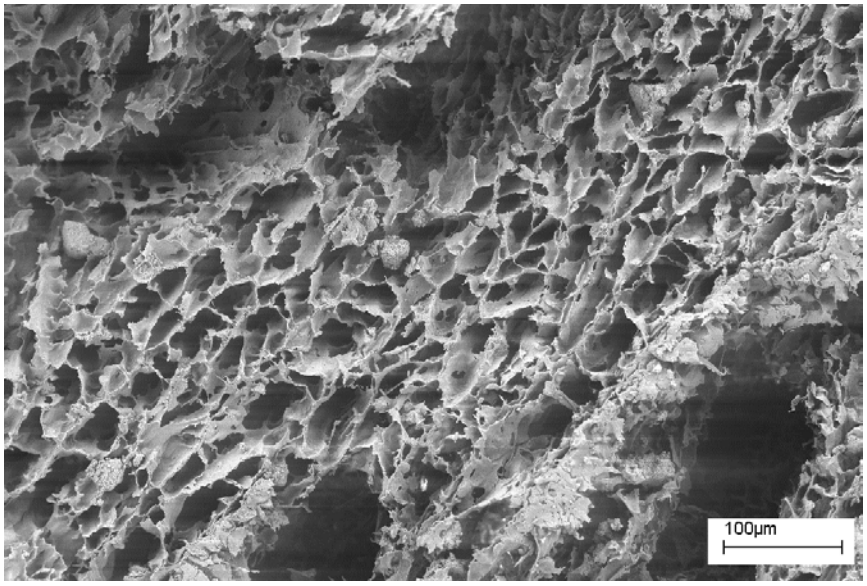

(b)

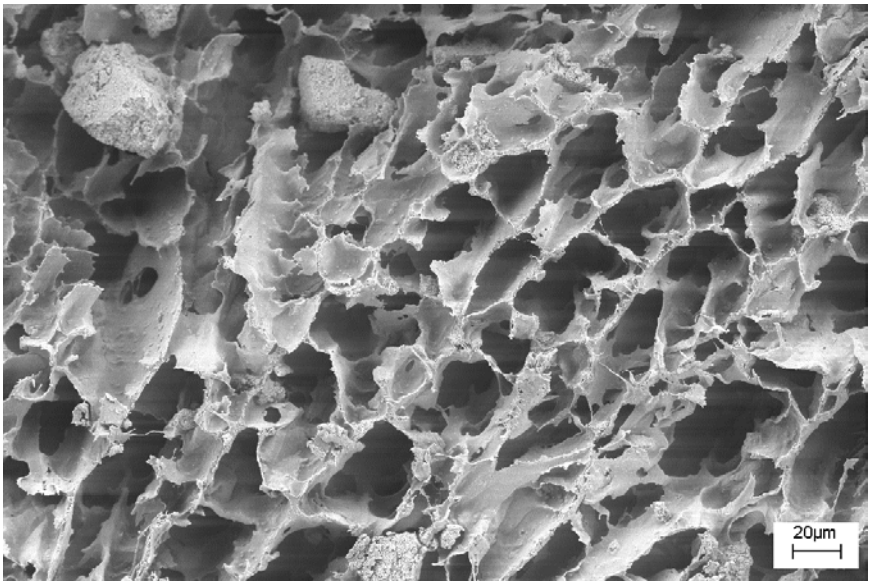

Figure 7

(c)

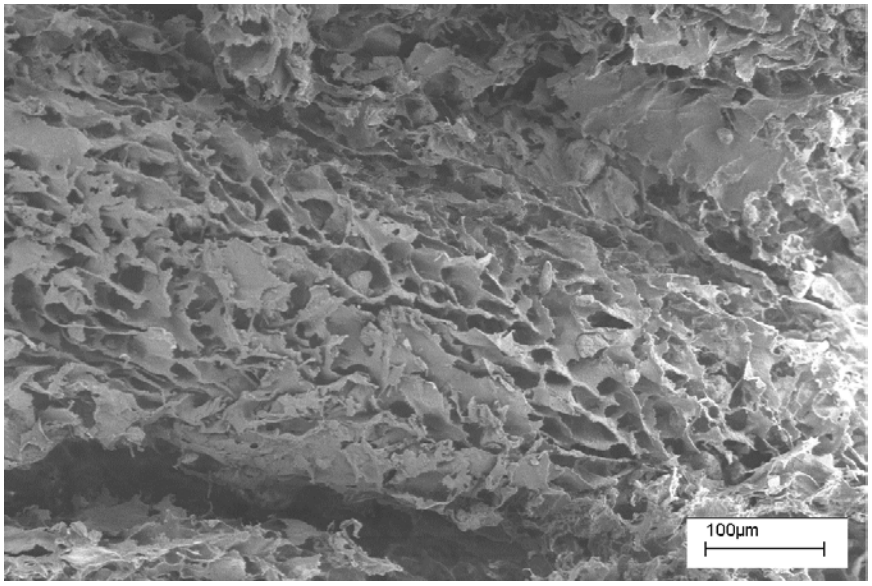

(d)

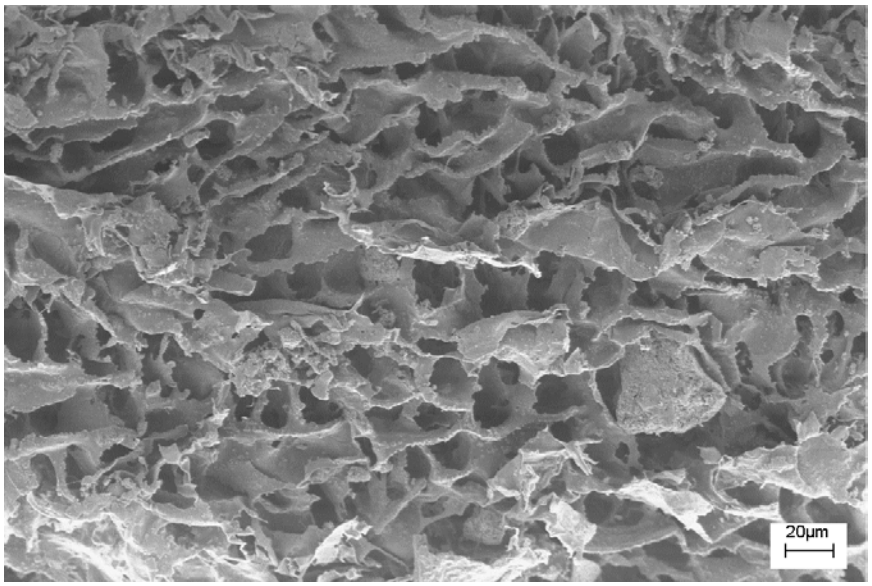

Figure 8

(a)

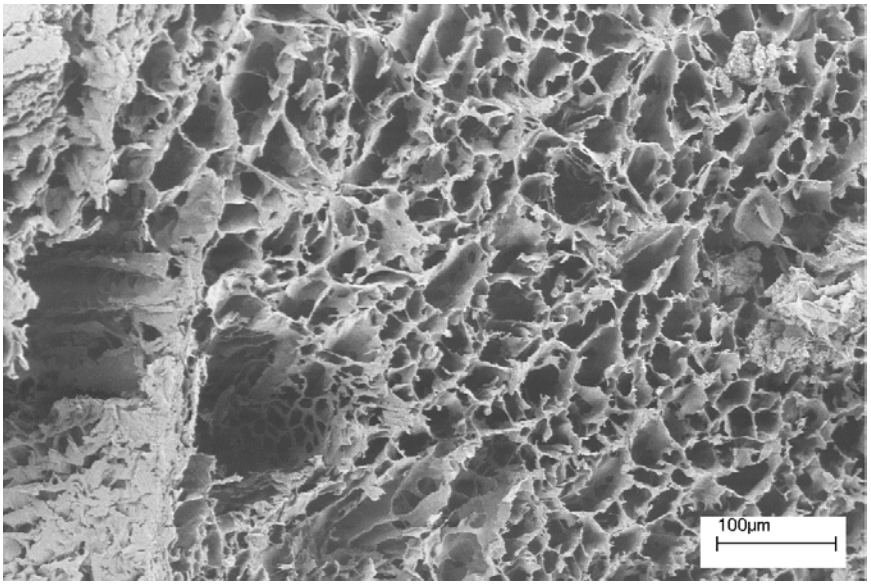

(b)

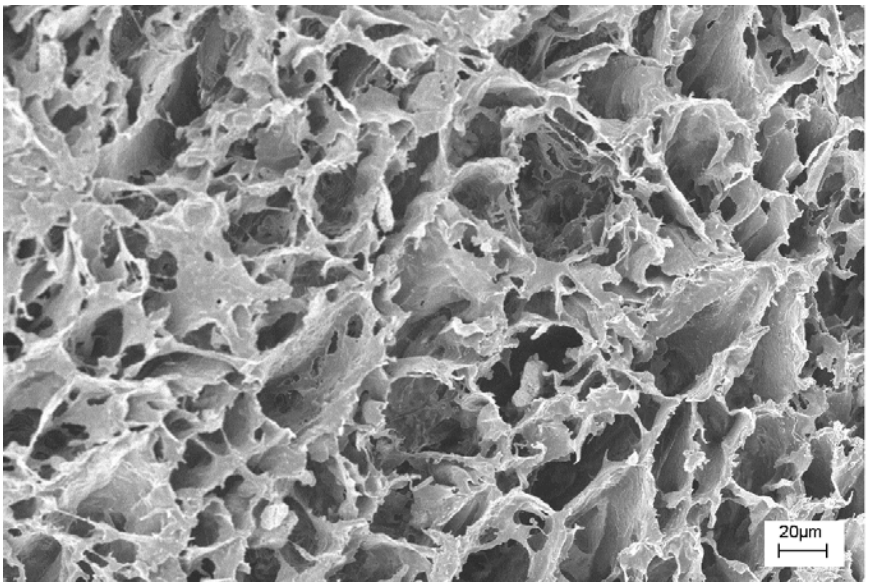

Figure 8

(c)

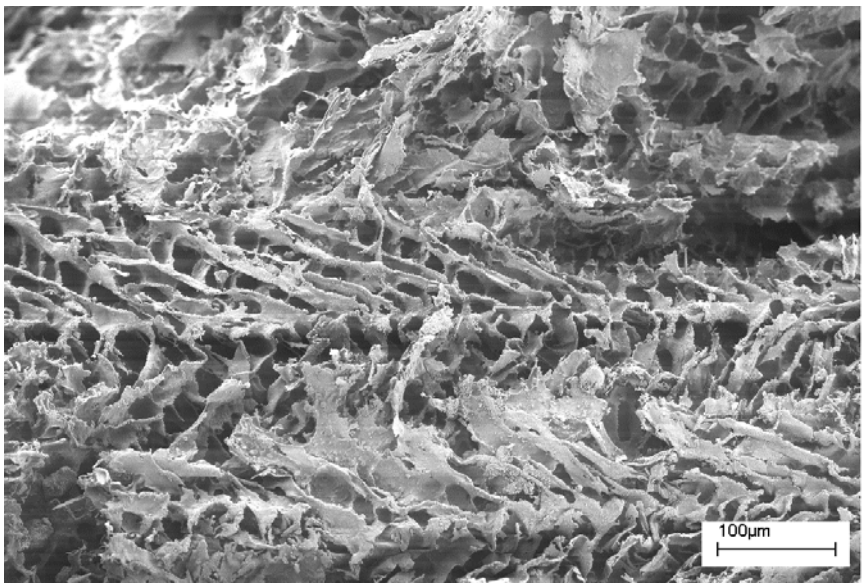

(d)

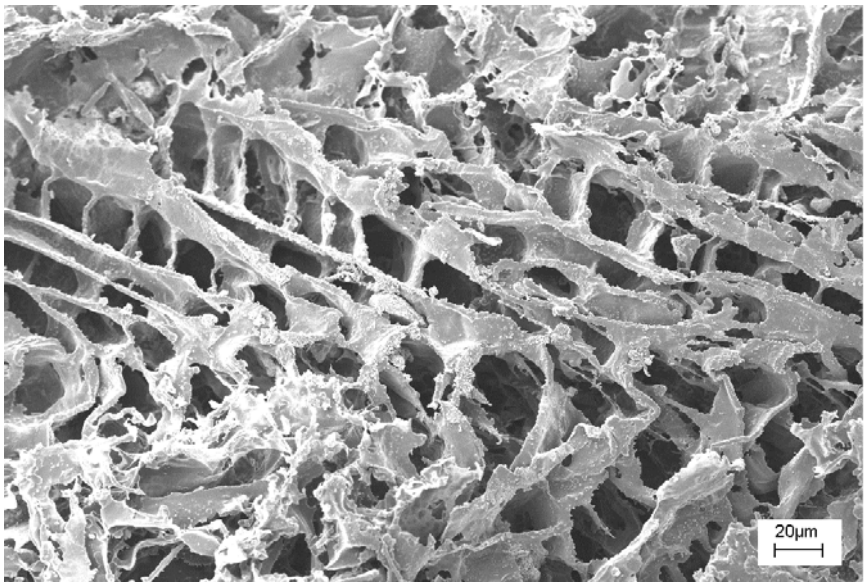

Figure 9

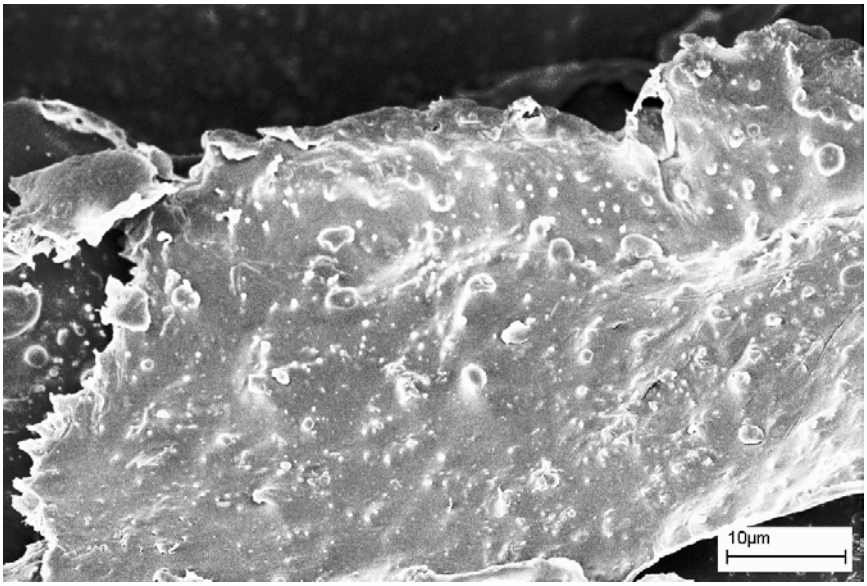

Figure 10

(a)

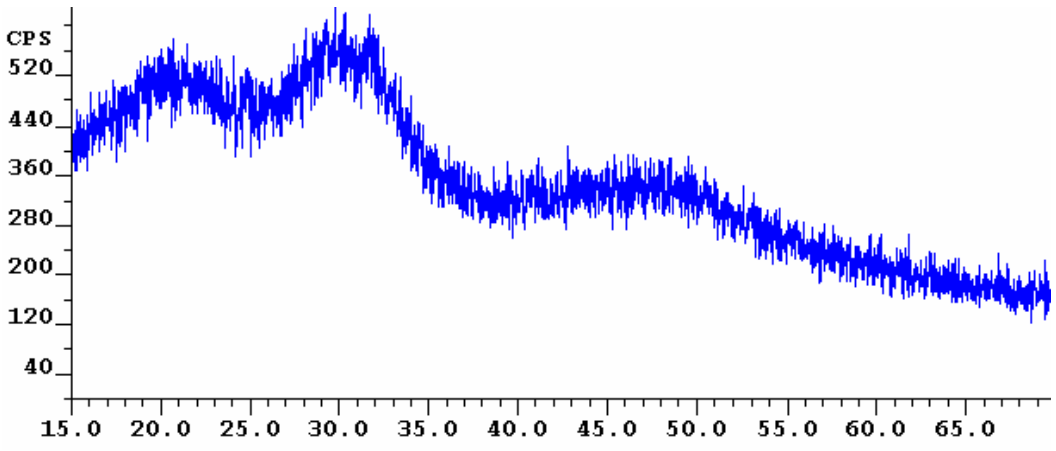
CPS
520
440
360
280
200
120
40
15.0 20.0 25.0 30.0 35.0 40.0 45.0 50.0 55.0 60.0 65.0
2-Theta (degrees)

(b)

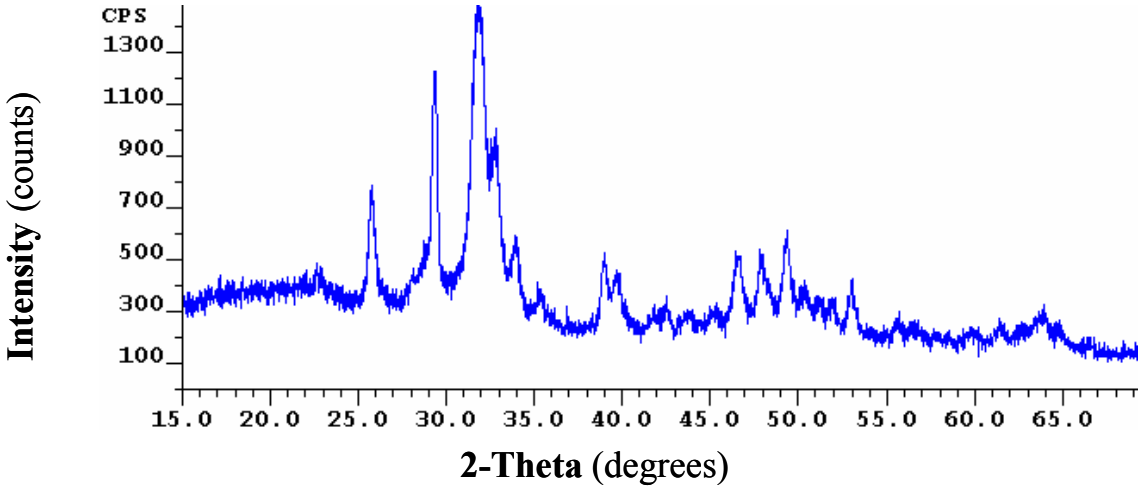
CPS
1300
1100
900
700
500
300
100
Intensity (counts)
15.0 20.0 25.0 30.0 35.0 40.0 45.0 50.0 55.0 60.0 65.0
2-Theta (degrees)

Figure 11

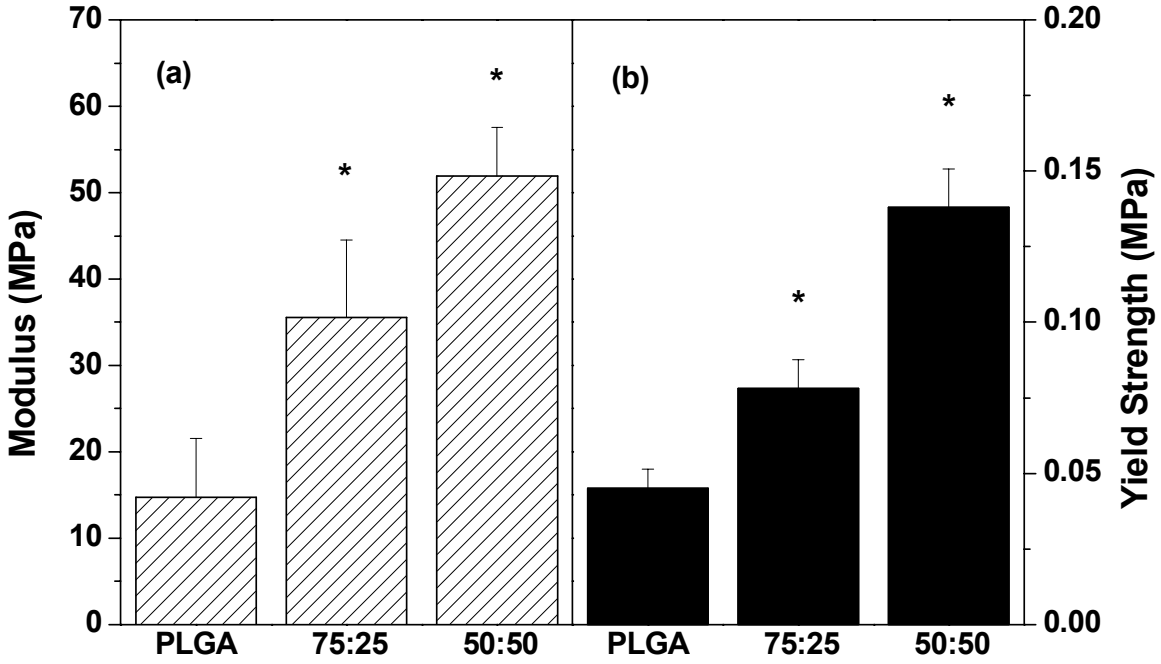
(a)
(b)
Modulus (MPa)
Yield Strength (MPa)
70
60
50
40
30
20
10
0
0.20
0.15
0.10
0.05
0.00
*
PLGA
75:25
50:50

Table 1

Scaffold	Max. pore diameter (μm)	Min. pore diameter (μm)	Average pore diameter (μm)
10% PLGA	114.7	3.3	20.9
5% PLGA	32.5	1.8	4.3
10% PLGA/Zr-ACP 75:25	154.4	3.6	46.8
5% PLGA/Zr-ACP 75:25	107.2	2.9	26.8
10% PLGA/Zr-ACP 50:50	26.5	1.9	6.2
5% PLGA/Zr-ACP 50:50	18.4	1.3	3.2
10% PLGA/HAP 75:25	34.8	2.6	6.4
5% PLGA/HAP 75:25	10.4	0.35	2.5
10% PLGA/HAP 50:50	41.5	2	9.5
5% PLGA/HAP 50:50	27.3	1.1	5.5

Chapter 4: Conclusions and Future Work

4.1 Conclusions

The main goals of this research were to determine the osteogenic nature of Zr-ACP and to incorporate Zr-ACP into a resorbable PLGA porous structure to use as a scaffold for bone tissue engineering. To accomplish these goals, MC3T3-E1 cells were cultured in the presence of Zr-ACP to determine cell response determined by changes in DNA synthesis, alkaline phosphatase activity, osteopontin synthesis and collagen synthesis. Next, porous PLGA/Zr-ACP composite foams were fabricated using a thermal phase inversion technique and were characterized by determining pore size, pore distribution, compressive yield and compressive modulus.

Results from Chapter 2 indicate that Zr-ACP increases osteoblast function by affecting proliferation, ALP activity, and ECM production of MC3T3-E1 cells. Specifically, Zr-ACP in cell culture did not inhibit DNA synthesis but actually increased DNA synthesis at days 11 and 14 as compared to the control. In addition, Zr-ACP had a stimulatory effect on cells to transiently increase cellular ALP activity when added at intermediate (day 4) and late stages (day 11) in culture. Zr-ACP also had an effect on the third stage of osteoblastic differentiation which is the matrix mineralization stage. A 2-fold increase in osteopontin synthesis was measured when Zr-ACP was added to culture at days 4 and 11. An increase in collagen synthesis was determined for cells with addition of Zr-ACP to cell culture at days 0, 4 and 11 although the increases were not statistically significant. These results indicate that Zr-ACP has an osteogenic potential in vitro and could increase osteogenesis when incorporated into a bone scaffold in vivo.

The results from Chapter 3 show that porous PLGA/Zr-ACP composite foams can be fabricated by employing a thermal phase inversion technique. Average pore diameter ranging from 3.6 μm to 154.4 μm was found for composites with 25% (w/v) Zr-ACP using a 10% (w/v) PLGA/dioxane mixture. This pore size range is on the lower end of suggested pore sizes for biodegradable bone scaffolds (150 μm to 700 μm) [1]. Compressive modulus and yield strength was increased significantly with addition of 50% (w/v) to the PLGA scaffold. Furthermore, XRD analysis confirmed that Zr-ACP retained its amorphous structure during composite fabrication. This is important because the amorphous structure of Zr-ACP is thought to increase dissolution rates, ion release and subsequently enhance osteoblast differentiation in vitro.

4.2 Future Work

Zr-ACP was introduced into cell culture at a concentration of 5mg/ml for the studies in Chapter 2. It would be interesting to vary concentration of Zr-ACP in culture to determine the threshold value for significant cell response. This study would help determine the optimal amount of Zr-ACP to be added into PLGA scaffolds to elicit a favorable cell response. Also, different formulations of Zr-ACP could be synthesized (changes in Zr content) to vary release rate of calcium and phosphate ions. It would also be valuable to determine the amount of Zr-ACP that converts to HAP in these in vitro experiments. Other more specific bone marker proteins, such as osteocalcin and bone sialoprotein, could be assayed to more definitively determine osteoblast differentiation in response to Zr-ACP in vitro. Also, other materials such as β-TCP could be used as controls for the studies presented in Chapter 2. This extra control would add breadth to

the study and allow for comparison between Zr-ACP and other ceramics that have been added to biodegradable scaffolds.

With regards to scaffold fabrication, phase inversion temperature could be varied to modulate pore size and pore wall thickness. Previous studies have shown that a quench temperature of $0^{o}C$ is sufficient to obtain pore sizes on the range of 250 μm in a 10% (w/v) PLGA/dioxane solution [2]. Increasing the phase inversion temperature from $-50^{o}C$ to $0^{o}C$ could possibly increase average pore size and wall thickness in a 10% (w/v) PLGA/dioxane solution with 25 wt% Zr-ACP. To determine porosity of the scaffolds, mercury intrusion porosimitry (MIP) could be employed. In the MIP method, mercury is forced to penetrate into porous samples under stringently controlled pressures to give data on the volume and size of the pores and the density of the composite. If pores are found to be non-interconnected, then different processing techniques, such as gas foaming, should be employed in addition to TIPS to meet the requirement of interconnected pores.

Ultimately, the goal of this research was to produce a bone scaffold that promotes osteogenesis in vivo. Once the optimum scaffold porosity and morphology is obtained, in vitro and in vivo bone scaffold testing would be required. Scaffolds would be seeded with MC3T3-E1 cells or BMSC's in vitro and subsequent cell assays (including DNA synthesis, ALP activity, and various ECM synthesis) would be completed to determine scaffold capability. Finally, it would be beneficial to conduct in vivo testing by implanting seeded scaffold into animals with critical size defects. The ability for scaffolds to heal critical size defects by forming new bone formation in animals is necessary for scaffold incorporation into humans.

4.3 References

[1] Ishaug-Riley SL, Crane-Kruger GM, Yaszemski MJ, Mikos AG. Three-dimensional culture of rat calvarial osteoblasts in porous biodegradable polymers. Biomaterials 1998;19:1405-1412.

[2] Zhang RY, Ma PX. Poly(alpha-hydroxyl acids) hydroxyapatite porous composites for bone-tissue engineering. I. Preparation and morphology. Journal of Biomedical Materials Research 1999;44:446-455.

Vita

Bryce Matthew Whited was born in the spring of 1980 in Parkersburg, WV. He graduated from Parkersburg High school in 1998 and enrolled at Virginia Polytechnic Institute and State University. Five years later, in 2003, he earned his Bachelor's degree in Materials Science and Engineering. In August 2003, Bryce continued his education at Virginia Tech pursuing a Master's degree in Biomedical Engineering. After earning his M.S. degree, Bryce plans to go to Maracaibo, Venezuela to do missionary work with Campus Crusade for Christ.